Supporting Information

Gem-diprenylation of acylphloroglucinols by a fungal prenyltransferase of the dimethylallyltryptophan synthase superfamily

Kang Zhou,[†] Carsten Wunsch, [†] Jungui Dai, [‡] and Shu-Ming Li [*†]

[†]*Pharmazeutische Biologie und Biotechnologie, Philipps-Universität Marburg, Robert-Koch-Str. 4, 35037, Marburg, Germany*

[‡]*State Key Laboratory of Bioactive Substance and Function of Natural Medicines, Institute of Materia Medica, Chinese Academy of Medical Sciences and Peking Union Medical College, Xian Nong Tan Street, Beijing 100050, China*

** Fax:, 49-6421-2825365; Tel:, 49-6421-2822461*

Shu-Ming Li: shuming.li@staff.uni-marburg.de

I. Experimental Section

Chemicals

DMAPP, GPP, and FPP were synthesized according to the method described for GPP reported previously.[1] Phlorisobutyrophenone (PIBP, **1**), phlorisovalerophenone (PIVP, **2**), and phlorbenzophenone (PBZP, **3**) were synthesized according to protocols described previously.[2]

Cultivation of *Aspergillus terreus* for DNA isolation

A. terreus DSM 1958 was purchased from German Collection of Microorganisms and Cell Cultures (DSMZ) and cultivated in 300 mL cylindrical flasks containing 100 mL YME medium (yeast extract: 4.0 g L^{-1}, glucose monohydrate: 4.0 g L^{-1}, and malt extract: 10.0 g L^{-1}) at 30 °C for 5 days in darkness for DNA isolation.

DNA propagation in *E. coli* and DNA isolation from fungi

Standard procedures for DNA isolation and manipulation in *E. coli* were performed as described.[3] To isolate genomic DNA from *A. terreus*, the mycelia of a 5 day-old culture were collected and washed with phosphate-buffered saline consisting of 137 mM NaCl, 2.7 mM KCl, 1 mM Na_2HPO_4, and 0.18 mM KH_2PO_4, pH 7.3. Genomic DNA was isolated according to a method described previously.[4]

Amplification of sequence coding forAtaPT (accession number KP893683) orthologue from *A. terreus* DSM 1958

The ATEG_04999 orthologue is composed of two exons of 1148 and 127 bp, interrupted by an intron of 48 bp. The two exons were amplified separately by PCR in a first round and then combined in a second round by using the PCR products from the first round as templates and primers. The High Fidelity PCR kit (Roche) was used for this purpose. Two primers CaW_04999-1 (5´-AA***G***CATGCTCCCCCCATCAGACAGC-3´) and CaW_04999-3 (5´-TTCTTGGTTTGCGAGATATCCACATTGGGAAATTTCGCCTTGAGTTCATC-3´) were used for amplification of the first exon and CaW_04999-2 (5´-GATGAACTCAAGGCGAAATTTCCCAATGTGGATATCTCGCAAACCAAGAA-3´) and CaW_04999-4 (5´-CC***GG***ATC***C***CACACGTGCGACATTTC-3´) for the second exon. Bold letters in CaW_04999-1 and CaW_04999-4 represent mutations inserted into the original genome sequence in order to create the restriction sites SphI and BamHI for cloning in pQE-70. The underlined letters in CaW_04999-2 and CaW_04999-3 indicate overlapping sequences for fusion.

Gene cloning, overproduction and purification of AtaPT

The generated PCR fragment consisting of the coding region was cloned in pGEM-T Easy and sequenced. After confirming the sequence, the insert was released by restriction with SphI/BamHI and recloned in pQE-70 vector, resulted in the construct pCaW7 for expression in *E. coli*.
For AtaPT overproduction with pCaW7, *E.coli* M15 [pREP] cells were cultivated as described previously.[5] Protein purification was carried out according to the procedure described by Yin et al.[5] The purity of the obtained protein was proven on SDS-PAGE (Figure S1).

Enzyme assays

The enzyme assays (100 µL) contained 1 mM of acylphloroglucinols **1**, **2**, or **3**, 5 mM of $CaCl_2$, 2 mM of DMAPP, GPP or FPP, 0.2–5.0 % of glycerol, 5 % of DMSO, and 20 µg or 50 µg of purified recombinant protein in 50 mM of Tris-HCl, pH 7.5. The reaction mixtures were incubated at 37 °C for 2 h and terminated by addition of 100 µL methanol. The proteins were removed by centrifugation at 13,000 rpm for 20 min. The supernatants were analyzed on HPLC described below. For analysis on LC-MS, the reaction mixtures were extracted four times with double volumes of ethyl acetate. The organic phases were combined and evaporated under reduced pressure to afford the residues, which were dissolved in 100 µL methanol and analyzed on LC-MS.

Assays for isolation of the enzyme products were carried out in large scales (20–30 mL) containing 1 mM of acylphloroglucinols, 2 mM of DMAPP, GPP or FPP, 5 mM of $CaCl_2$, 0.2–5.0 % of glycerol, 5 % of DMSO, 10–20 mg of recombinant protein in 50 mM of Tris-HCl, pH 7.5. After incubation at 37 °C for 16 h, the reaction mixtures were extracted four times with double volumes of ethyl acetate. The organic phases were combined and evaporated. The residues were dissolved in 0.5–1.0 mL of methanol and purified on a preparative HPLC column.

Assays for determination of the kinetic parameters of acceptors (100 µL) contained 5 mM of $CaCl_2$, 0.2–5.0 % of glycerol, 5% of DMSO, 2 mM of DMAPP, GPP or FPP, **1**, **2**, and **3** at final concentrations of up to 5.0 mM and different amounts of proteins in 50 mM of Tris-HCl, pH 7.5 (Table S8). For determination of the kinetic parameters of the prenyl donors DMAPP and GPP, **1** or **3** at a final concentration of 1 mM, DMAPP of up to 1.0 mM and GPP of up to 4.0 mM were used. Higher DMAPP and GPP concentrations led to inhibition of the AtaPT reactions. The used protein amounts are given in Table S8. The reaction mixtures were incubated within the linear range of the product formation for different times (Table S8 and Figures S32-42) and terminated with 100 µL methanol. Proteins were removed by centrifugation at 13,000 rpm for 20 min and the supernatants were analyzed on HPLC.

Ion dependence of the AtaPT reaction

To determine the ion dependency of AtaPT, incubations with different cations, including Mn^{2+}, Mg^{2+}, Ca^{2+}, Ni^{2+}, Fe^{2+}, Zn^{2+}, Co^{2+}, Cu^{2+}, Na^{+}, and K^{+} at 5 mM, were carried out in the presence of **1** and DMAPP. The 100 µL reaction mixtures contained 50 µg of AtaPT-His_6, 2 mM of DMAPP, 1 mM of **1** and were incubated at 37 °C for 2 h. Incubations with EDTA and without additives were used as controls. As shown in Figure S2, different ions had various contributions to the catalytic activity. In comparison to the assay without additives, addition of EDTA did not influence the enzyme activity. Ca^{2+} and Mg^{2+} enhanced the enzyme activity slightly. Ca^{2+} was therefore used in all enzyme assays in this study.

Analysis of enzyme products by HPLC, LC-MS, and NMR

Agilent HPLC series 1200 (Böblingen, Germany) alone and with a micrOTOF-Q III spectrometer with an ESI source (Bruker, Bremen, Germany) were used for analysis of the enzyme products. Analysis of the enzyme products on HPLC without the spectrometer was performed on an Agilent Eclipse XDB-C_{18} column (4.6 × 150mm, 5 µm) with a linear gradient of 10–100 % acetonitrile in water in 40 min and a flow rate at 0.5 mL/min. The column was then washed with acetonitrile for 5 min and equilibrated with 5 % acetonitrile in water for 5 min. The HPLC chromatograms of incubation mixtures of **1**, **2**, and **3** with AtaPT or AnaPT in the presence of DMAPP, GPP or FPP are shown as Figures S3-S5.

Analysis of the enzyme products on LC-MS was carried out on a CS Multospher 120 RP 18 column (2 × 250mm, 5 µm) and a linear gradient of 5–100 % acetonitrile in water, both containing 0.1% formic acid, in 40 min and a flow rate at 0.25 mL/min. The column was then washed with 100 % acetonitrile containing 0.1% formic acid for 5 min and equilibrated with 5 %, acetonitrile in water for 5 min. The parameters of the spectrometer were set as following: electrospray positive ion mode for ionization, capillary voltage with 4.5kV, collision energy with 8.0eV.The LC-MS chromatograms of the incubation mixtures of **1**, **2**, and **3** with AtaPT in the presence of DMAPP, GPP or FPP are provided as Figures 2–3 in the main text. HR-ESI-MS data are given in Table S1.

The enzyme products were isolated on HPLC with an Agilent Eclipse XDB-C18 column (9.4× 250 mm, 5 µm) with a linear gradient of 30–100 % acetonitrile in water in 30 min and a flow rate at 2.0 mL/min. After each run, the column was equilibrated with 10 % acetonitrile in water for 10 min.

^{1}H NMR spectra were recorded at room temperature on an ECA- 400 or an ECX-500 spectrometer (JEOL, Tokyo, Japan). Chemical shifts were referenced to the solvent signal at 2.05 ppm for acetone-D_6 and 7.26 ppm for $CHCl_3$. All spectra were processed with MestReNova 5.2.2 (Metrelab Research,

Santiago de Compostella, Spain). NMR spectra and data of the prenylated products are provided as Figures S6-S29 and Tables S2-S7, respectively.

Structure elucidation

Inspection of the ^{1}HNMR spectra of the isolated products indicated the regular attachment of the prenyl moieties, i.e. *via* their C-1, to three different kinds of atoms, which can be clearly distinguished by the chemical shifts of H´-1 of the prenyl chains (d, 2H, $-CH_2-$). The signals of this proton of *O*-prenylated derivatives are strongly downfield shifted to the range of 4.5-4.7 ppm.[6] Chemical shifts between 3.2–3.4 ppm are characteristic for H´-1 of the prenyl moieties attached to an aromatic *C*-atom.[2] The signals at about 2.5 ppm are those attached to sp^3 *C*-atoms.

By comparison of NMR data in the literature, the monoprenylated derivatives **1D1**,[2] **2D1**,[2] **3D1**,[2] **1D2**,[7] **1G1**,[8] **2G1**,[8] **3G1**,[9] **1G2**,[10] **3G2**,[7] **1F1**,[11,9] and **3F1**[9] were identified unequivocally. As reported previously, the *gem*-diprenylated derivative **1D3** exists as a mixtures of four tautomeric forms in $CDCl_3$[12]. The ^{1}H NMR spectrum of **1D3** in $CDCl_3$ obtained in this study corresponded very well to that in the literature.[12] Existence of tautomeric forms in $CDCl_3$ was also observed for **2D3** and **3D3** **(**data not shown). Using acetone-D_6 as solvent, the tautomers of **1D3**, **2D3**, and **3D3** illustrated in Scheme 2 are predominant structures. The NMR data of **2D3** and **3D3** are consistent very well with those reported previously.[13,14]

The structures of **2D2**, **2D4**, **2G2**, **2F1**, **1F2**, **2F2**, and **3F2** have not been reported prior to this study. The *O*-monoprenylated products **2D2**, **2G2**, **1F2**, **2F2**, and **3F2** carry their prenyl moieties at the *para*-position of the acyl residues, which are proven by the identical resonance of H-3 and H-5. The structure of **2F1** was elucidated by comparison with those of **1F1**. Only one singlet for an aromatic proton at δ5.89 ppm was found in the ^{1}H NMR spectrum of **2D4**. The signals of the two dimethylallyl moieties correspond well to those in **2D1** and **2D2**, respectively, indicating *C*- and *O*-prenylation. In addition, the $[M+H]^+$ ion of this product is 136 Da larger than that of **2**, confirming the diprenylation of **2**. Conversion of **2D1** to **2D3** and **2D4** by AtaPT provided additional evidence for the structure of **2D4**.

Time dependence of the formation of 2D1 and 2D3 in the reaction mixture of 2 as well as 3D1 and 3D3 in the reaction mixture of 3

To determine the relationship of **2D1** and **2D3** in the reaction mixtures (100 µL) of **2** with AtaPT, time dependence of their formation was determined with 0.5 mM of **2** and 50 µg of AtaPT in the presence of 2 mM of DMAPP. As shown in Figure S30, formation of **2D1** reached its maximal after incubation for 30 min and decreased slowly during further incubations. After incubation for 480 min,

only 12.8% of the maximal value was detected for **2D1**. In contrast, the formation of **2D3** increased continuously during incubation up to 480 min.

In analogy to **2**, **3** was also incubated with AtaPT and DMAPP for different times. As shown in Figure S31, similar results were obtained for the formation of **3D1** and **3D3**. The changes are somewhat slowly than those in the incubation of **2**. The product yield of 3**D1** reached its maximal at 60 min and decreased after 180 min. The formation of **3D3** increased continuously during the whole incubation process. These results confirmed that **2D3** and **3D3** are formed from **2** and **3** *via* **2D1** and **3D1**, respectively.

II. References

(1) Woodside, A. B.; Huang, Z.; Poulter, C. D. *Org. Synth.* **1988**, *66*, 211.
(2) Zhou, K.; Ludwig, L.; Li, S.-M. *J. Nat. Prod.* **2015**, *78*, 929.
(3) Sambrook, J.; Russell, D. W. *Molecular cloning: a laboratory manual;* 3rd ed.; Cold Spring Harbor Laboratory Press, Cold Spring Harbor: New York, 2001.
(4) Yu, X.; Li, S.-M. *Methods Enzymol.* **2012**, *516*, 259.
(5) Yin, W.-B.; Grundmann, A.; Cheng, J.; Li, S.-M. *J. Biol. Chem.* **2009**, *284*, 100.
(6) Zou, H.-X.; Xie, X.; Zheng, X.-D.; Li, S.-M. *Appl. Microbiol. Biotechnol.* **2011**, *89*, 1443.
(7) Bohlmann, F.; Suwita, A. *Phytochemistry* **1978**, *17*, 1929.
(8) Rios, M. Y.; Delgado, G. *Phytochemistry* **1992**, *31*, 3491.
(9) Wang, X.; Lee, Y. R. *Tetrahedron* **2011**, *67*, 9179.
(10) Bohlmann, F.; Mahanta, P. K. *Phytochemistry* **1979**, *18*, 348.
(11) Yu, Q.; Ravn, R. R.; Jacob, M. R.; Khan, S. I.; Agarwal, A. K.; Yu, B. Y.; Li, X. C. *J. Nat. Prod.* **2016**, *79*, 2195.
(12) George, J.-H.; Hesse, M.-D.; Baldwin, E.; dlington, R.-M. *Org. Lett.* **2010**, *12*, 3532.
(13) Mizobuchi, S.; Sato, Y. *Agricultural and Biological Chemistry* **1985**, *49*, 399.
(14) Cann, M. R.; Davis, A. M.; Shannon, P. V. R. *J. Chem. Soc. , Perkin Trans. 1* **1984**, 1413.

III. Table of HR-ESI-MS data

Table S1. HR-ESI-MS data of enzyme products

Product	Chemical formula	HR-ESI-MS data		
		Calculated $[M+H]^+$	**Measured $[M+H]^+$**	**Deviation [ppm]**
1D1	$C_{15}H_{21}O_4$	265.1434	265.1428	2.3
1D2	$C_{15}H_{21}O_4$	265.1434	265.1414	7.5
1D3	$C_{20}H_{29}O_4$	333.2060	333.2057	0.9
1D4	$C_{20}H_{29}O_4$	333.2060	333.2052	2.4
2D1	$C_{16}H_{23}O_4$	279.1591	279.1587	1.4
2D2	$C_{16}H_{23}O_4$	279.1591	279.1577	5.0
2D3	$C_{21}H_{31}O_4$	347.2217	347.2217	0.1
2D4	$C_{21}H_{31}O_4$	347.2217	347.2213	1.2
3D1	$C_{18}H_{19}O_4$	299.1278	299.1270	2.7
3D3	$C_{23}H_{27}O_4$	367.1904	367.1902	0.5
3D4	$C_{23}H_{27}O_4$	367.1904	367.1885	5.2
1G1	$C_{20}H_{29}O_4$	333.2060	333.2047	3.9
1G2	$C_{20}H_{29}O_4$	333.2060	333.2063	-0.9
2G1	$C_{21}H_{31}O_4$	347.2217	347.2220	-0.9
2G2	$C_{21}H_{31}O_4$	347.2217	347.2204	3.7
3G1	$C_{23}H_{27}O_4$	367.1904	367.1926	-6.0
3G2	$C_{23}H_{27}O_4$	367.1904	367.1900	1.1
1F1	$C_{25}H_{37}O_4$	401.2686	401.2669	4.2
1F2	$C_{25}H_{37}O_4$	401.2686	401.2680	1.5
2F1	$C_{26}H_{39}O_4$	415.2843	415.2849	-1.4
2F2	$C_{26}H_{39}O_4$	415.2843	415.2840	0.7
3F1	$C_{28}H_{35}O_4$	435.2530	435.2503	6.2
3F2	$C_{28}H_{35}O_4$	435.2530	435.2527	0.7

IV. Tables of NMR data

Table S2. ^{1}H-NMR data of the enzyme products **1D1**, **2D1**, **3D1**, **1D2**, and **2D2**, 500 MHz.

Comp	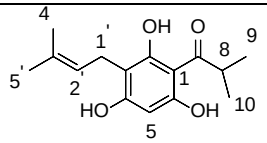 **1D1**	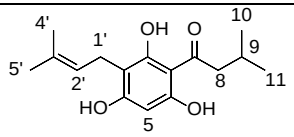 **2D1**	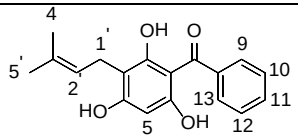 **3D1**	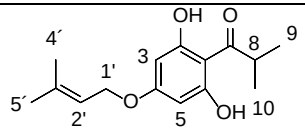 **1D2**		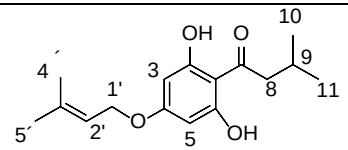 **2D2**	
Solvent	acetone-D_6	acetone-D_6	acetone-D_6	acetone-D_6	$CDCl_3$	acetone-D_6	$CDCl_3$
Pos.	δ_H, *J* in Hz	$\delta_{H,}$(*J* in Hz	$\delta_{H,}$, *J* in Hz	$\delta_{H,}$, *J* in Hz	$\delta_{H,}$, *J* in Hz	$\delta_{H,}$, *J* in Hz	$\delta_{H,}$, *J* in Hz
3	/	/	/	6.00, s	5.93, s	5.99, s	5.92, s
5	6.06, s	6.07, s	6.04, s	6.00, s	5.93, s	5.99, s	5.92, s
6	/	/	/	/	/	/	/
8	3.98, sept, 6.7	2.94, d, 6.7	/	3.98, sept, 6.8	3.85, sept, 6.8	2.96, d, 6.7	2.93, d, 6.7
9	1.13, d, 6.7	2.24, m	7.60, dt, 7.2, 1.3	1.13, d, 6.8	1.17, d, 6.8	2.24, m	2.25, m
10	1.13, d, 6.7	0.95, d, 6.7	7.43, br t, 7.2	1.13, d, 6.8	1.17, d, 6.8	0.95, d, 6.7	0.97, d, 6.7
11	/	0.95, d, 6.7	7.48, tt, 7.2, 1.3	/	/	0.95, d, 6.7	0.97, d, 6.7
12	/	/	7.43, br t, 7.2	/	/	/	/
13	/	/	7.60, dt, 7.2, 1.3	/	/	/	/
1´	3.23, d, 7.2	3.23, d, 7.2	3.29, d, 7.2	4.56, d, 6.7	4.49, d, 6.9	4.55, d, 6.7	4.49, d, 6.8
2´	5.22, tsept, 7.2, 1.4	5.22, tsept, 7.2, 1.4	5.27, tsept, 7.2, 1.4	5.42, tsept, 6.7, 1.5	5.44, br t, 6.9	5.42, br t, 6.7	5.42,br t, 6.8
4´	1.62, s	1.62, s	1.65, s	1.74, s	1.73, s	1.74, s	1.73, s
5´	1.73, s	1.73, s	1.76, s	1.77, s	1.79, s	1.77, s	1.79, s
OH	14.12, s	14.09, s	12.21, s	11.84, s	/	11.83, s	/
OH	9.48, s	9.54, s	9.19, s	/	/	/	/
OH	9.06, s	9.12, s	8.93, s	/	/	/	/

Table S3. ^{1}H-NMR data of the enzyme products **1D3**, **2D3**, **3D3**, and **2D4**, 500 MHz

Comp	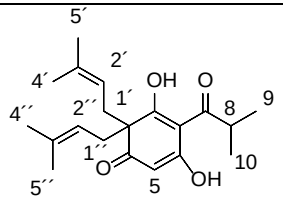 **1D3**	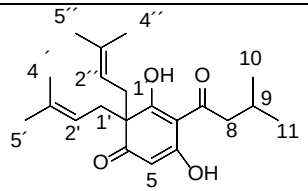 **2D3**	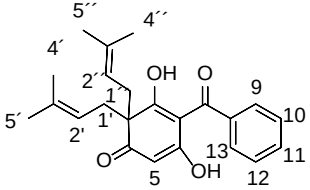 **3D3**	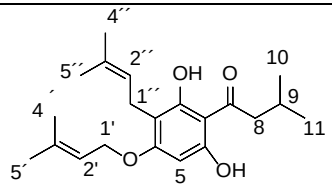 **2D4**	
Solvent	acetone-D_6	acetone-D_6	acetone-D_6	acetone-D_6	$CDCl_3$
Pos.	δ_H, *J* in Hz	δ_H, *J* in Hz	δ_H, *J* in Hz	δ_H, *J* in Hz	δ_H, *J* in Hz
5	5.58, s	5.60, s	5.73, s	6.11, s	5.89, s
8	4.00, sept, 6.8	2.80 [a]	/	2.80 [a]	2.87, d, 6.7
9	1.03, d, 6.8	2.04, m	7.44, br t, 7.4	2.04, m,	2.17, m
10	1.03, d, 6.8	0.94, d, 6.7	7.37, br t, 7.4	0.94, d, 6.7	0.94, d, 6.7
11	/	0.94, d, 6.7	7.46, br t, 7.4	0.94, d, 6.7	0.94, d, 6.7
12	/	/	7.37, br t, 7.4	/	/
13	/	/	7.44, br t, 7.4	/	/
1´	2.51, dd, 13.5, 7.5 2.65, dd, 13.5, 7.5	2.53, dd, 13.2, 7.5 2.65, dd, 13.2, 7.5	2.55, dd, 13.6, 7.2 2.62, dd, 13.6, 7.2	4.57, d, 7.1	4.50, d, 7.1
2´	4.87, tsept, 7.5, 1.5	4.88, br t, 7.5	5.00, br t, 7.2	5.56, br t, 7.1	5.51, br t, 7.1
4´	1.52, s	1.54, s	1.65, s	1.74, s	1.74, s
5´	1.55, s	1.57, s	1.76, s	1.80, s	1.80, s
1´´	2.51, dd, 13.5, 7.5 2.65, dd, 13.5, 7.5	2.53, dd, 13.2, 7.5 2.65, dd, 13.2, 7.5	2.55, dd, 13.6, 7.2 2.62, dd, 13.6, 7.2	3.25, d, 7.2	3.37, d, 7.0
2´´	4.87, tsept, 7.5, 1.5	4.88, br t, 7.5	5.00, br t, 7.2	5.22, br t, 7.2	5.27, br t, 7.0
4´´	1.52, s	1.54, s	1.60, s	1.62, s	1.62, s
5´´	1.55, s	1.57, s	1.62, s	1.74, s	1.74, s
OH	/	/	/	14.4, s	14.6, s

[a] overlapping with signals of water

Table S4. ^{1}H-NMR data of the enzyme products **1G1**, **2G1**, and **3G1** in $CDCl_3$, 400 MHz

Comp	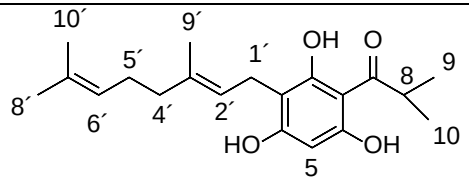 **1G1**	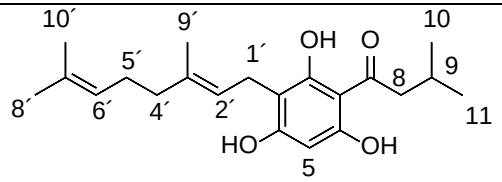 **2G1**	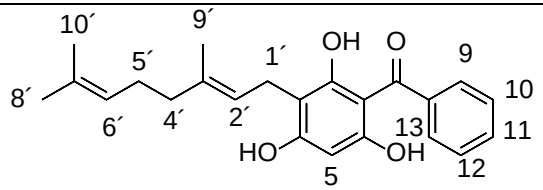 **3G1**
Pos.	δ_H, *J* in Hz	δ_H, *J* in Hz	δ_H, *J* in Hz
5	5.83, s	5.82, s	5.94, s
8	3.86, sept, 6.8	2.93, d, 6.7	/
9	1.17, d, 6.8	2.25, m	7.65, dt, 7.2, 1.2
10	1.17, d, 6.8	0.97, d, 6.7	7.52, br t, 7.2
11	/	0.97, d, 6.7	7.59, tt, 7.2, 1.2
12	/	/	7.52, br t, 7.2
13	/	/	7.65, dt, 7.2, 1.2
1´	3.38, d, 7.1	3.37, d, 7.1	3.38, d, 7.1
2´	5.25, br t, 7.1	5.25, br t, 7.1	5.27, br t, 7.1
4´	2.10, m	2.11, m	2.08, m
5´	2.10, m	2.11, m	2.08, m
6´	5.05, br t, 7.0	5.04, br t, 7.1	5.04, br t 7.1
8´	1.81, s	1.81, s	1.80, s
9´	1.67, s	1.68, s	1.66, s
10´	1.59, s	1.60, s	1.59, s

Table S5. ^{1}H-NMR data of the enzyme products **1G2**, **2G2**, and **3G2** in $CDCl_3$, 500 MHz

Comp	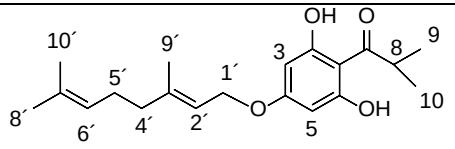 **1G2**	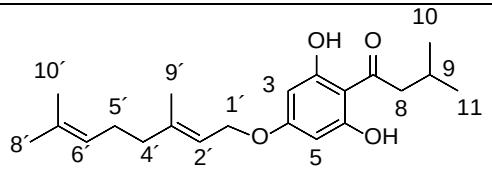 **2G2**	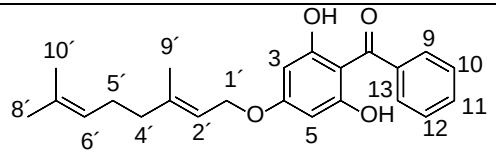 **3G2**
Pos.	δ_H, *J* in Hz	δ_H, *J* in Hz	δ_H, *J* in Hz
3	5.93, s	5.92, s	6.04, s
5	5.93, s	5.92, s	6.04, s
8	3.85, sept, 6.8	2.92, d, 6.7	/
9	1.17, d, 6.8	2.24, m	7.65, dt, 7.1, 1.4
10	1.17, d, 6.8	0.97, d, 6.7	7.54, br t, 7.1
11	/	0.97, d, 6.7	7.59, tt, 7.1, 1.4
12	/	/	7.54, br t, 7.1
13	/	/	7.65, dt, 7.1, 1.4
1´	4.52, d, 6.9	4.52, d, 6.9	4.56, d, 7.1
2´	5.43, br t, 6.9	5.43, br t, 6.9	5.46, br t, 7.1
4´	2.09, m	2.10, m	2.10, m
5´	2.09, m	2.10, m	2.10, m
6´	5.08, br t, 6.8	5.08, br t, 6.8	5.09, br t, 7.1
8´	1.72, s	1.72, s	1.74, s
9´	1.68, s	1.68, s	1.68, s
10´	1.60, s	1.60, s	1.61, s

Table S6. ^{1}H-NMR data of the enzyme products **1F1**, **2F1**, and **3F1** in acetone-D_6, 500 MHz

Comp	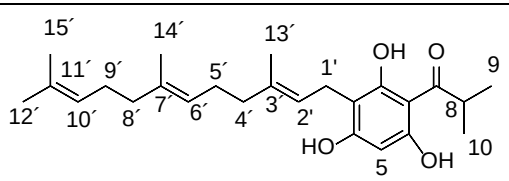 **1F1**	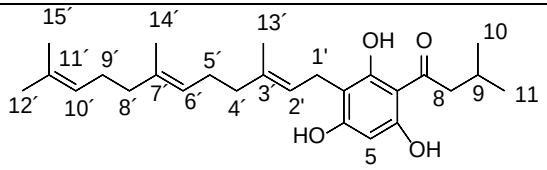 **2F1**	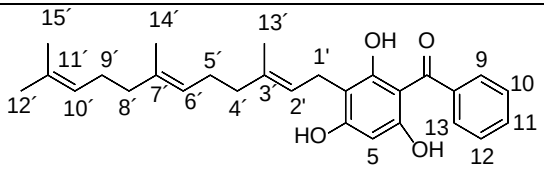 **3F1**
Pos.	δ_H, *J* in Hz	δ_H, *J* in Hz	δ_H, *J* in Hz
5	6.06, s	6.05, s	6.04, s
8	3.98, sept, 6.8	2.94, d, 6.7	/
9	1.13, d, 6.8	2.24, m	7.59, dt, 7.2, 1.4
10	1.13, d, 6.8	0.95, d, 6.7	7.40, br t, 7.2
11	/	0.95, d, 6.7	7.47, tt, 7.4, 1.4
12	/	/	7.40, br t, 7.2
13	/	/	7.59, dt, 7.2, 1.4
1´	3.25, d, 7.2	3.25, d, 7.2	3.31, d, 7.2
2´	5.25, br t, 7.2	5.25, br t, 7.2	5.30, br t, 7.2
4´	2.08, m	2.08, m	2.09, m
5´	2.08, m	2.08, m	2.09, m
6´	5.10, br t, 7.1	5.10, br t, 7.2	5.12, br t, 7.2
8´	1.93, m	1.97, m	1.97, m
9´	1.93, m	1.97, m	1.97, m
10´	5.07, br t, 7.1	5.07, br t, 7.2	5.08, br t, 7.2
12´	1.76, s	1.76, s	1.78, s
13´	1.64, s	1.64, s	1.64, s
14´	1.57, s	1.56, s	1.57, s
15´	1.57, s	1.56, s	1.57, s

Table S7. ^{1}H-NMR data of the enzyme products **1F2**, **2F2**, and **3F2** in acetone-D_6, 500 MHz

Comp	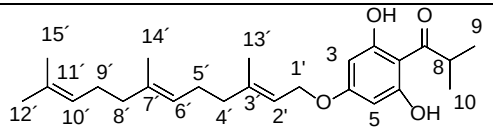 **1F2**	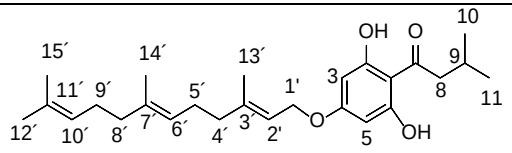 **2F2**	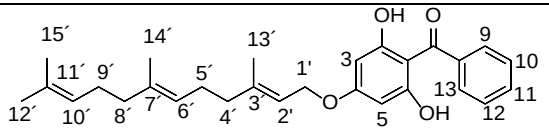 **3F2**
Pos.	δ_H, *J* in Hz	δ_H, *J* in Hz	δ_H, *J* in Hz
3	5.97, s	5.99, s	6.04, s
5	5.97, s	5.99, s	6.04, s
8	3.95, sept, 6.8	2.96, d, 6.7	/
9	1.11, d, 6.8	2.24, m	7.63, dt, 7.4, 1.4
10	1.11, d, 6.8	0.95, d, 6.7	7.42, br t, 7.4
11	/	0.95, d, 6.7	7.50, tt, 7.4, 1.4
12	/	/	7.42, br t, 7.4
13	/	/	7.63, dt, 7.4, 1.4
1´	4.57, d, 6.5	4.59, d, 6.6	4.63, d, 6.5
2´	5.41, br t, 6.5	5.43, br t, 6.6	5.46, br t, 6.5
4´	2.09, m	2.13, m	2.14, m
5´	2.09, m	2.13, m	2.14, m
6´	5.11, br t, 6.7	5.14, br t, 7.0	5.15, br t, 6.7
8´	1.94, m	1.97, s	1.98, m
9´	1.94, m	1.97, s	1.98, m
10´	5.06, br t, 6.9	5.09, br t, 7.0	5.10, br t, 6.9
12´	1.73, s	1.76, s	1.78, s
13´	1.62, s	1.65, s	1.65, s
14´	1.58, s	1.61, s	1.62, s
15´	1.55, s	1.58, s	1.58, s

V. Table of kinetic parameters

Table S8. Kinetic parameters of AtaPT toward **1**, **2**, **3**, DMAPP, and GPP

Prenyl donor	Prenyl acceptor	AtaPT: Protein amount and incubation time	AtaPT: K_M [mM]	AtaPT: k_{cat} [s^{-1}]	AtaPT: k_{cat}/K_M [$s^{-1}M^{-1}$]	AnaPT[a]: k_{cat}/K_M [$s^{-1}M^{-1}$]
Kinetic parameters of acceptors						
DMAPP	**1**	15μg, 20min	0.16 ± 0.006	0.284 ± 0.002	1775.0	54.5
	2	15μg , 90min	1.10 ± 0.035	0.103 ± 0.002	96.5	51.5
	3	15μg , 90min	0.58 ± 0.064	0.106 ± 0.005	182.8	62.5
GPP	**1**	15μg , 45min	1.27 ± 0.14	0.227 ± 0.001	178.7	/
	2	15μg, 30min	0.75 ± 0.008	0.197 ± 0.05	262.7	/
	3	15μg , 30min	0.47 ± 0.013	0.137 ± 0.0002	291.5	/
FPP	**1**	50μg, 90min	0.38 ± 0.027	0.014 ± 0.0003	36.8	/
	2	50μg, 90min	0.42 ± 0.04	0.012 ± 0.0007	28.6	/
	3	50μg , 90min	0.70 ± 0.12	0.012 ± 0.0007	17.1	/
Kinetic parameters of donors						
DMAPP	**1**	15μg, 20min	0.071 ± 0.0007	0.270 ± 0.0016	3816.9	40.0
GPP	**3**	15μg, 30min	0.46 ± 0.003	0.126 ± 0.0004	273.9	/

[a] Data adopted from Zhou, K.; Ludwig, L.; Li, S.-M. *J. Nat. Prod.* **2015**, *78*, 929

VI. Figure of SDS-PAGE

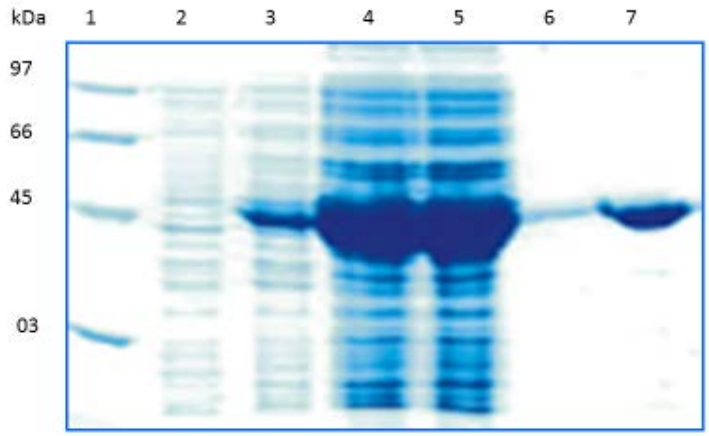

Figure S1. Monitoring of overproduction and purification of AtaPT. The proteins were separated on a 12 % polyacrylamide gel and stained with Coomassie brilliant blue R-250.

Lanes: 1, protein marker; 2, soluble fraction before induction; 3, soluble fraction after induction with 0.5 mM Isopropyl-β-D-thiogalactopyranoside at 37 °C for 6 h; 4, soluble protein fraction after centrifugation; 5, flow fraction; 6, washing fraction; 7, elution fraction.

VII. Graphical representation of the ion dependence of the AtaPT reaction

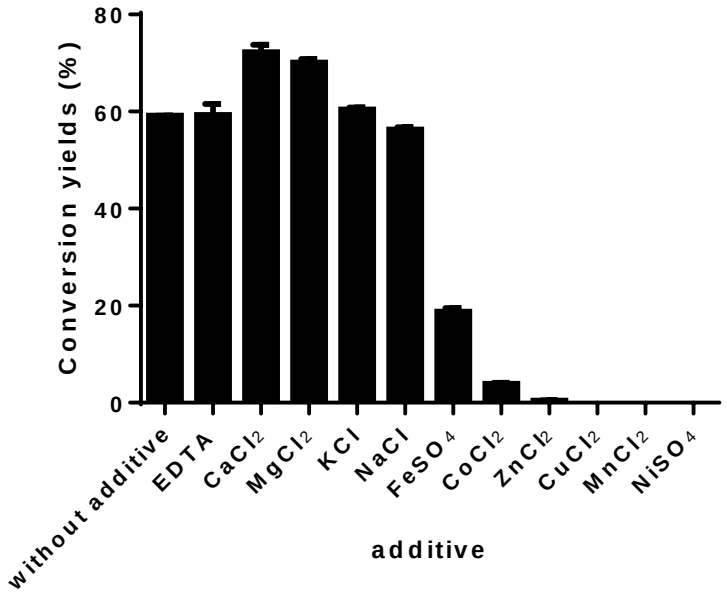

Figure S2. Dependence of the AtaPT reaction on the presence of ions. The reaction mixtures contained (100 µL) 50 µg of AtaPT-His_6, 5 mM of additives, 2 mM of DMAPP, 1 mM of **1** and were incubated at 37 °C for 2 h.

VIII. Figures for HPLC analysis of enzyme activities

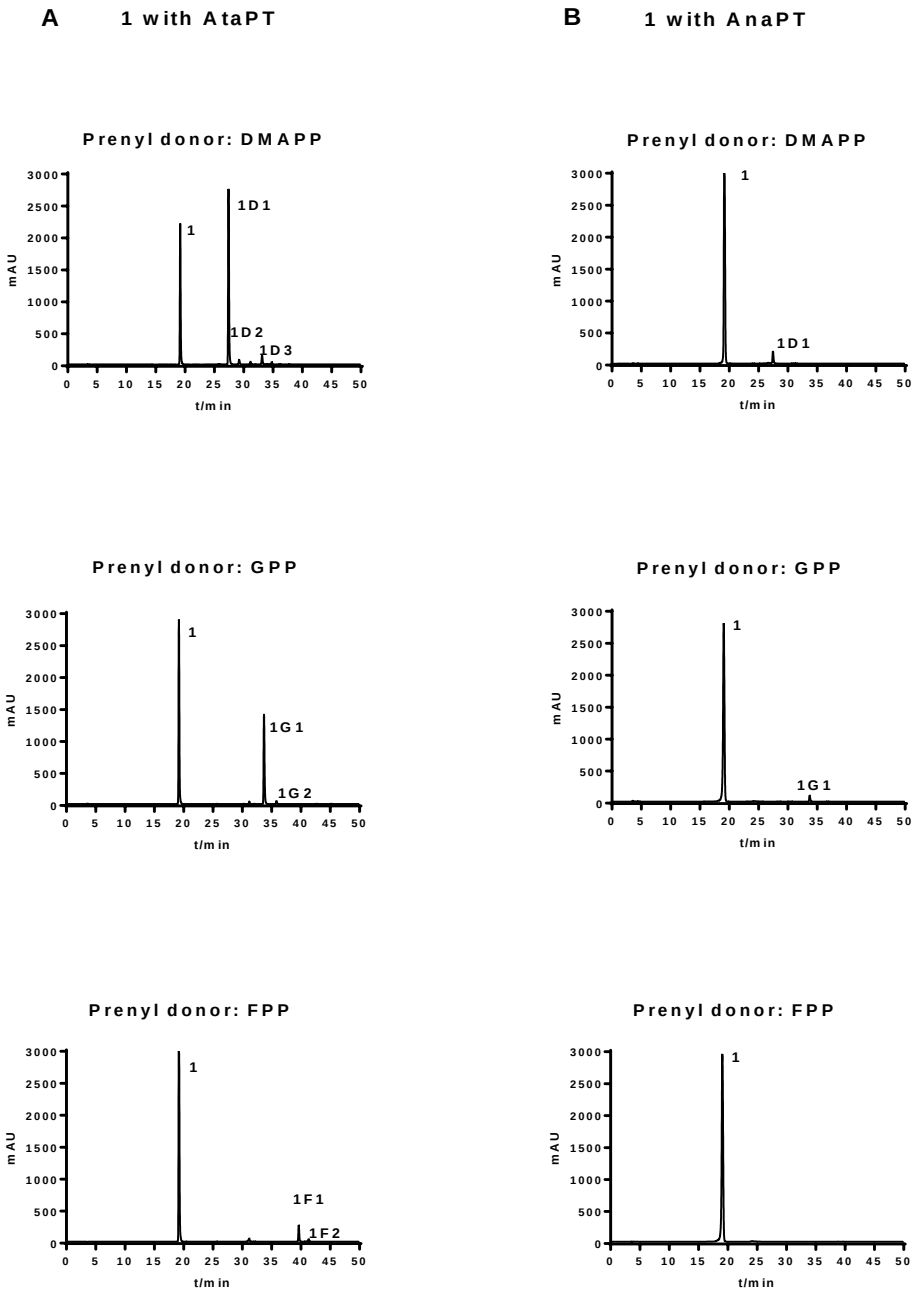

Figure S3. HPLC analysis of the reaction mixtures of **1** with AtaPT and AnaPT. The enzyme assays (100 μL) contained 1 mM of **1**, 5 mM of $CaCl_2$, 2 mM of DMAPP, GPP or FPP, 1.0−6.0% of glycerol (v/v), 5% of DMSO, (v/v), and 20 μg of the purified recombinant protein in 50 mM Tris-HCl, pH 7.5. The reaction mixtures were incubated at 37 °C for 2 h and detected with a diode assay detector. The absorption at 291 nm was used for illustration of the reaction with **1**.

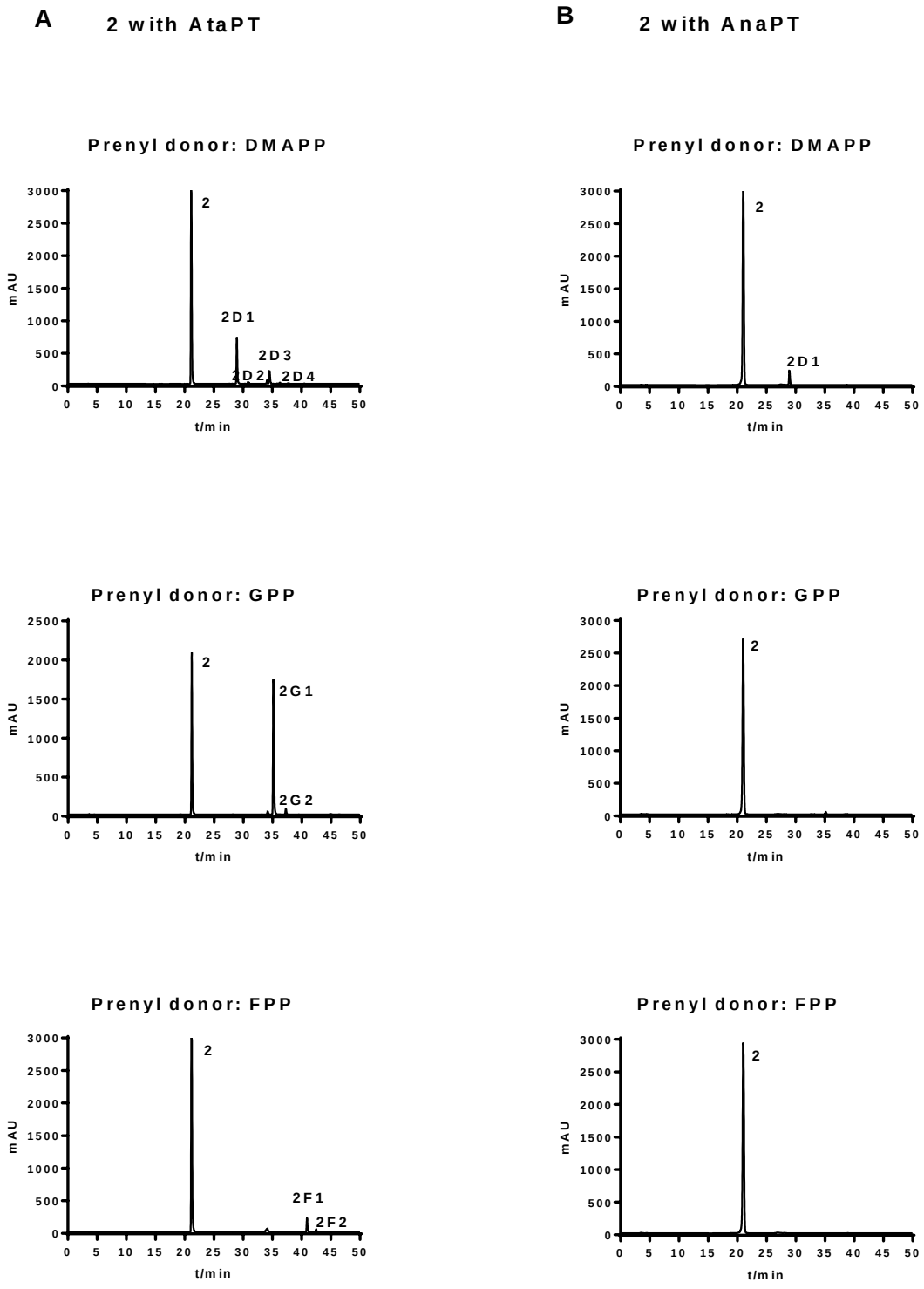

Figure S4. HPLC analysis of the reaction mixtures of **2** with AtaPT and AnaPT.

The enzyme assays (100 μL) contained 1 mM of **2**, 5 mM of $CaCl_2$, 2 mM of DMAPP, GPP or FPP, 1.0−6.0% of glycerol (v/v), 5% of DMSO (v/v), and 20 μg of the purified recombinant protein in 50 mM Tris-HCl, pH 7.5. The reaction mixtures were incubated at 37 °C for 2 h and detected with a diode assay detector. The absorption at 291 nm was used for illustration of the reaction with **2**.

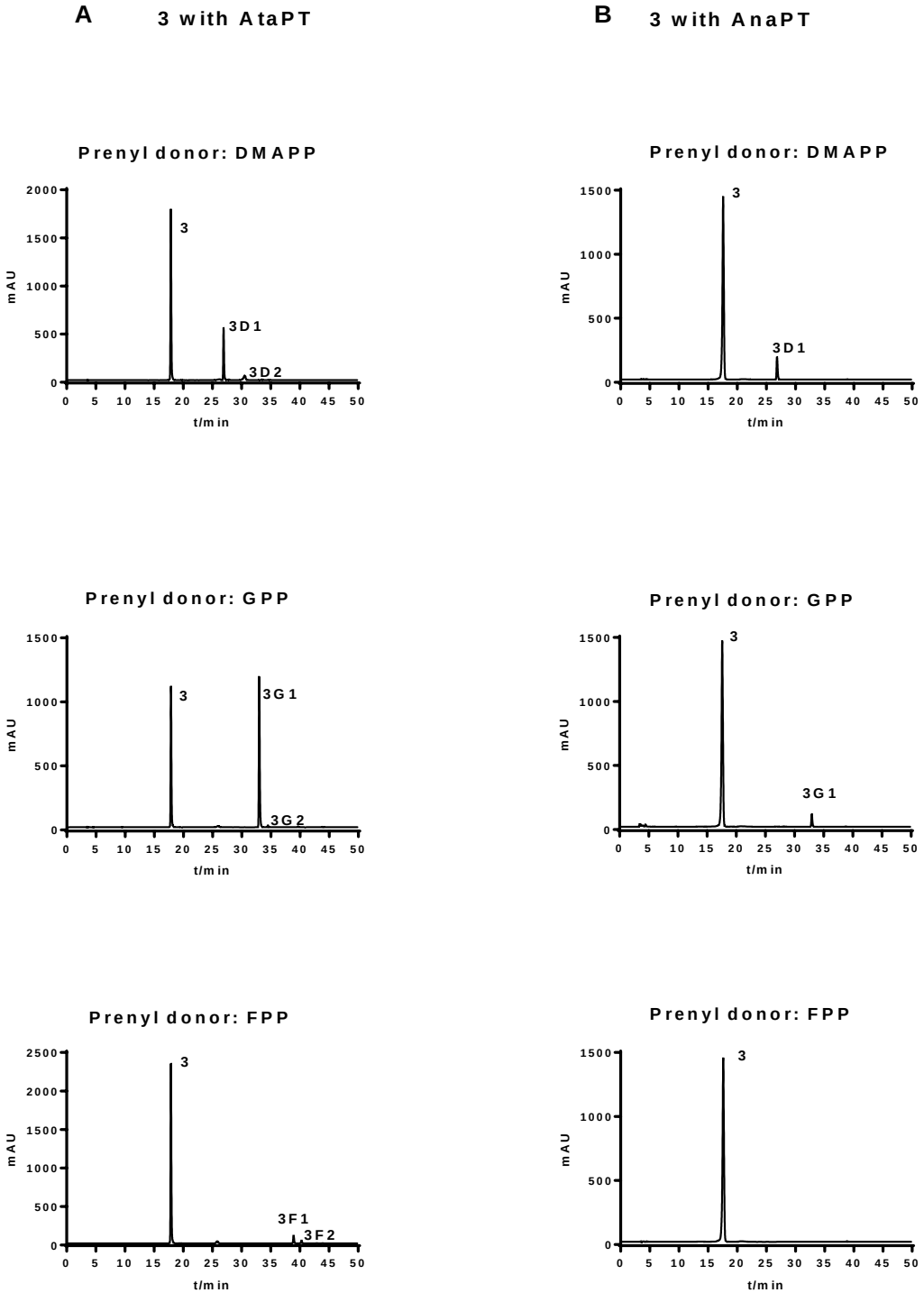

Figure S5. HPLC analysis of the reaction mixtures of **3** with AtaPT and AnaPT. T

The enzyme assays (100 μL) contained 1 mM of **3**, 5 mM of $CaCl_2$, 2 mM of DMAPP, GPP or FPP, 1.0−6.0% of glycerol (v/v), 5% of DMSO (v/v), and 20 μg of the purified recombinant protein in 50 mM Tris-HCl, pH 7.5. The reaction mixtures were incubated at 37 °C for 2 h and detected with a diode assay detector. The absorption at 306 nm was used for illustration of the reaction with **3**.

IX. Figures of NMR spectrum

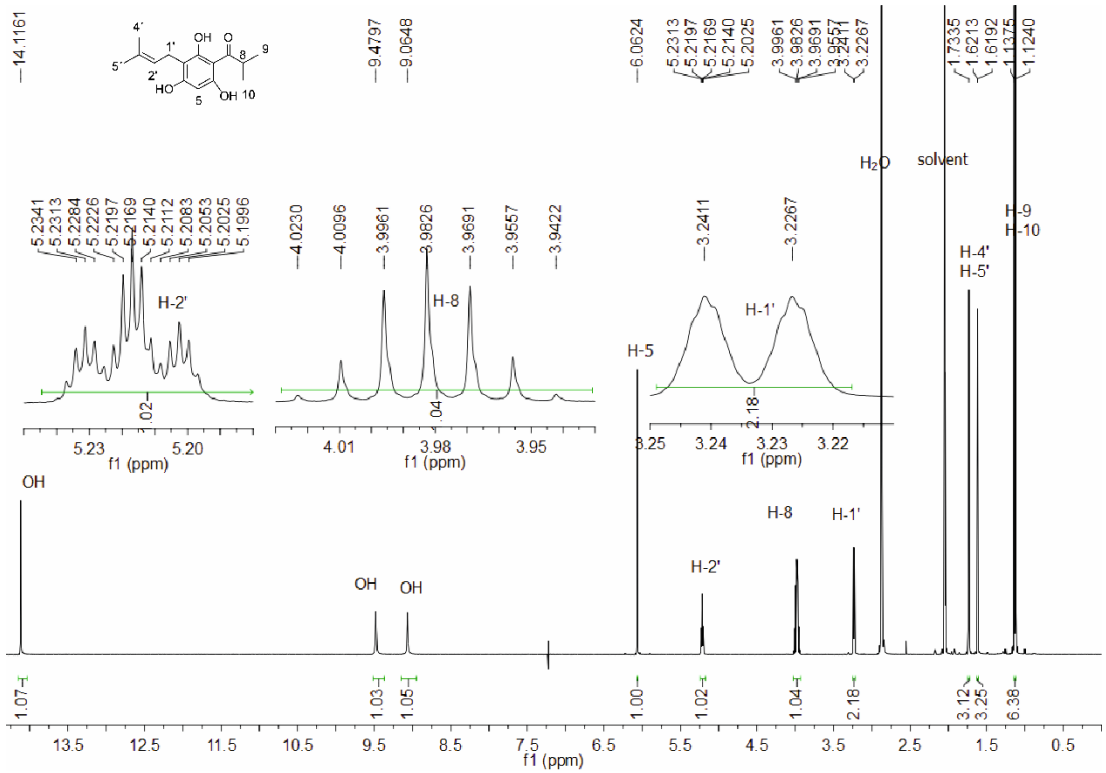

Figure S6. ^{1}H-NMR spectrum of **1D1** in acetone-D_6, 500 MHz.

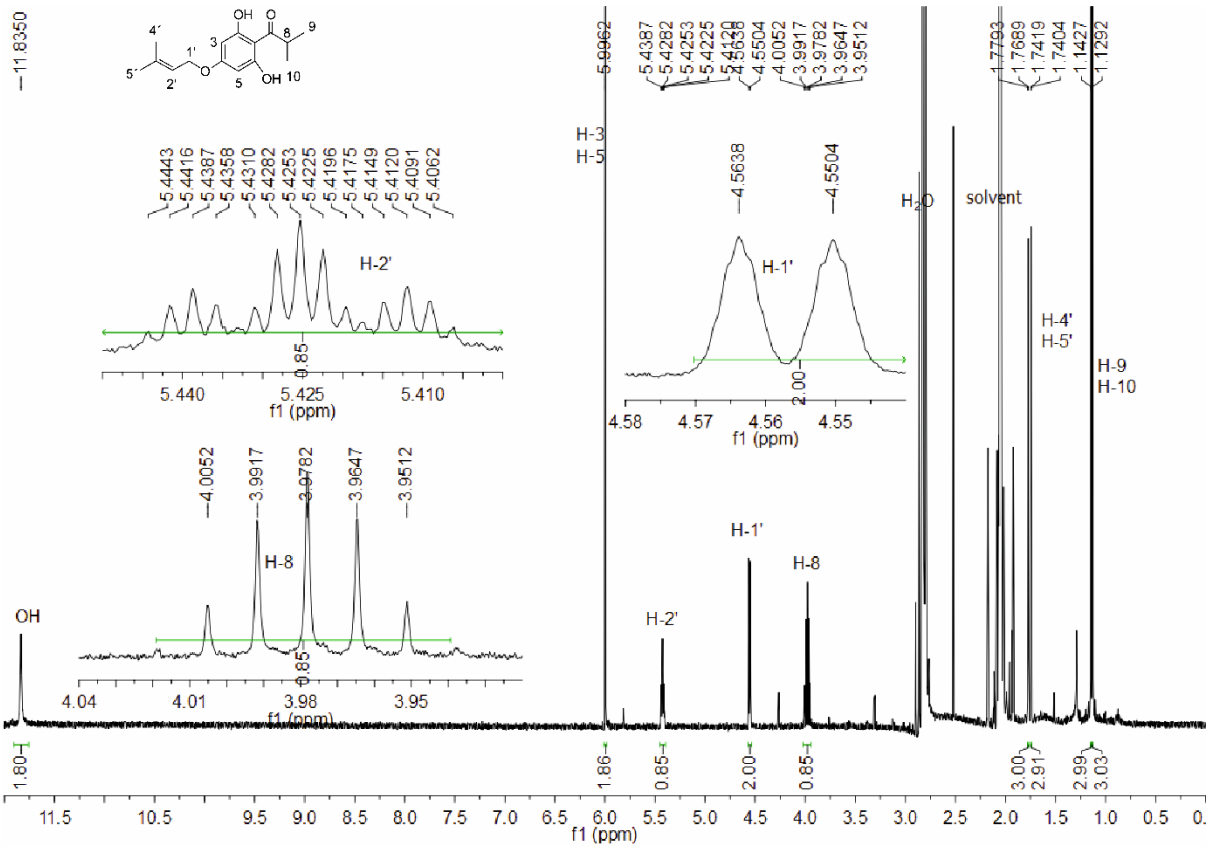

Figure S7. ^{1}H-NMR spectrum of **1D2** in acetone-D_6, 500 MHz.

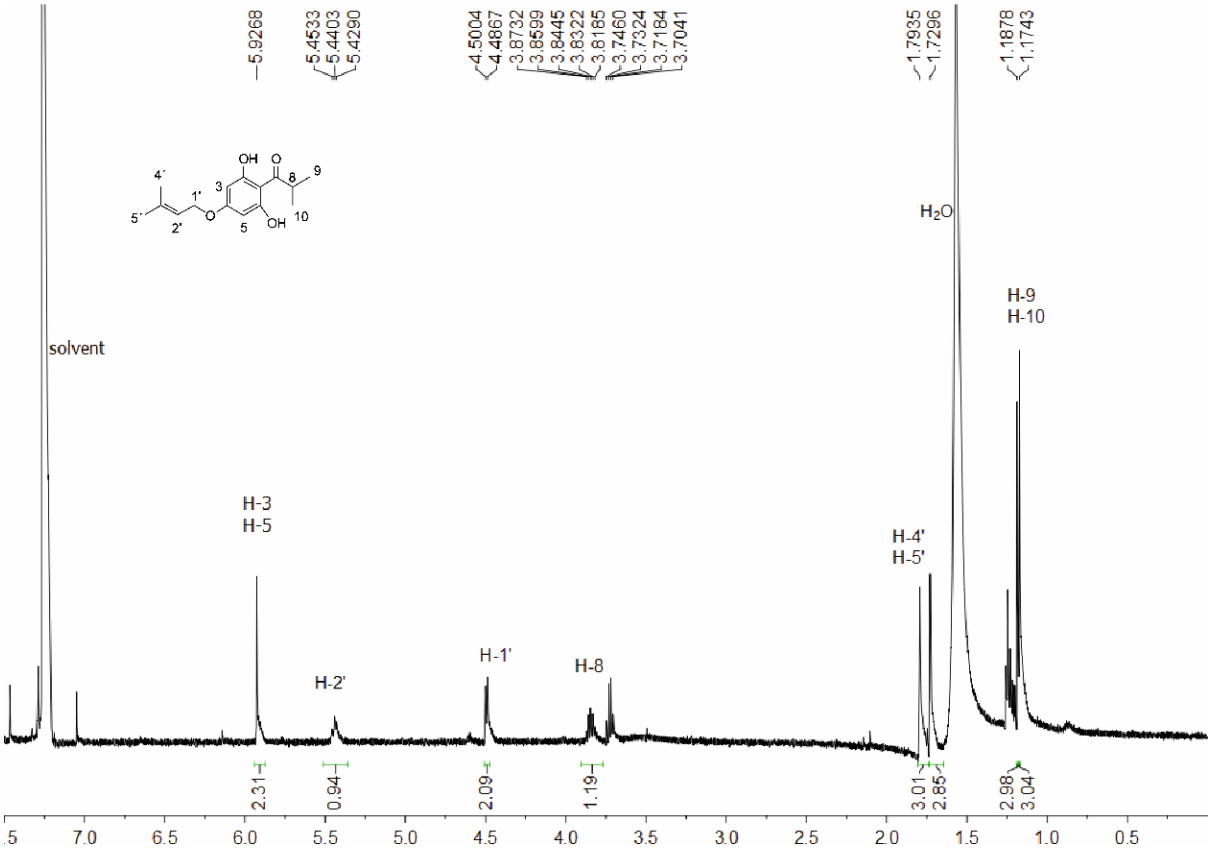

Figure S8. ^{1}H-NMR spectrum of **1D2** in $CDCl_3$, 500 MHz.

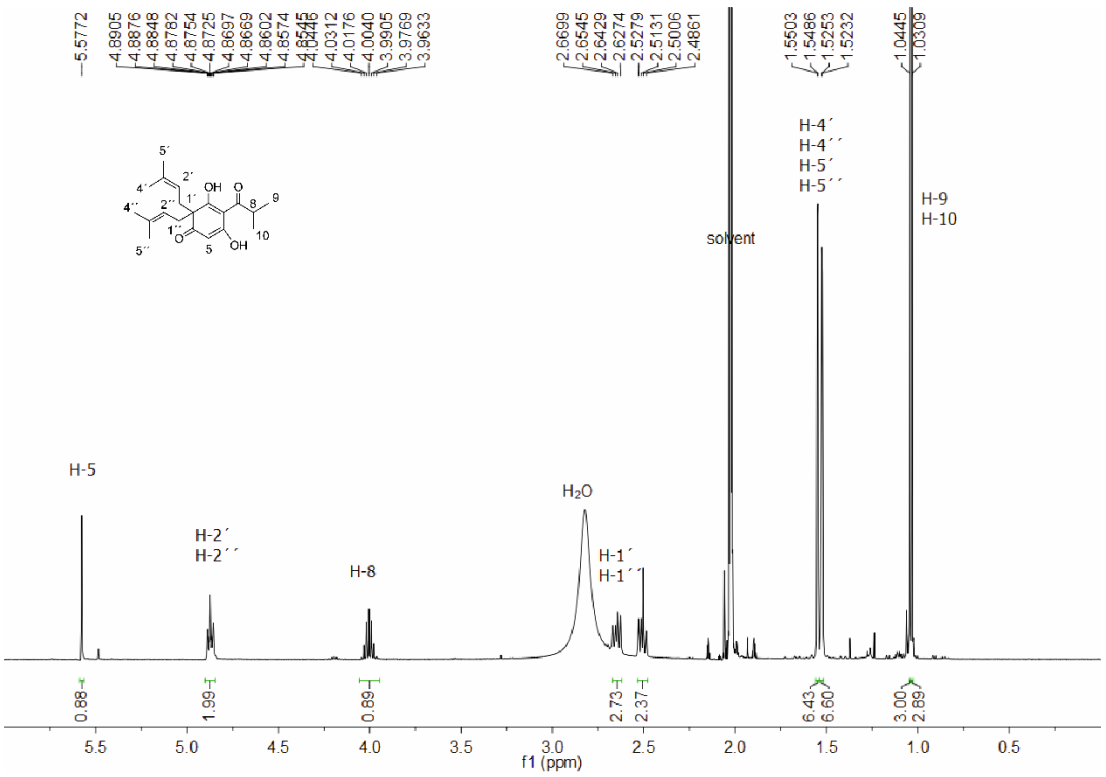

Figure S9. ^{1}H-NMR spectrum of **1D3** in acetone-D_6, 500 MHz.

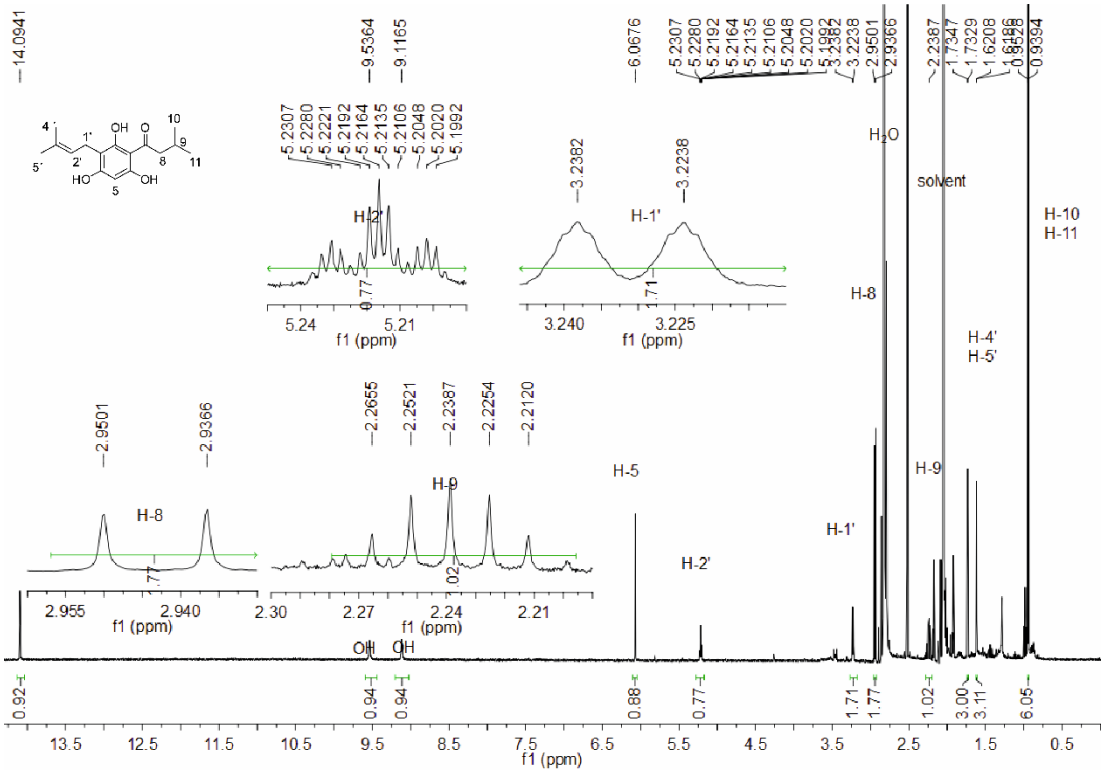

Figure S10. ^{1}H-NMR spectrum of **2D1** in acetone-D_6, 500 MHz.

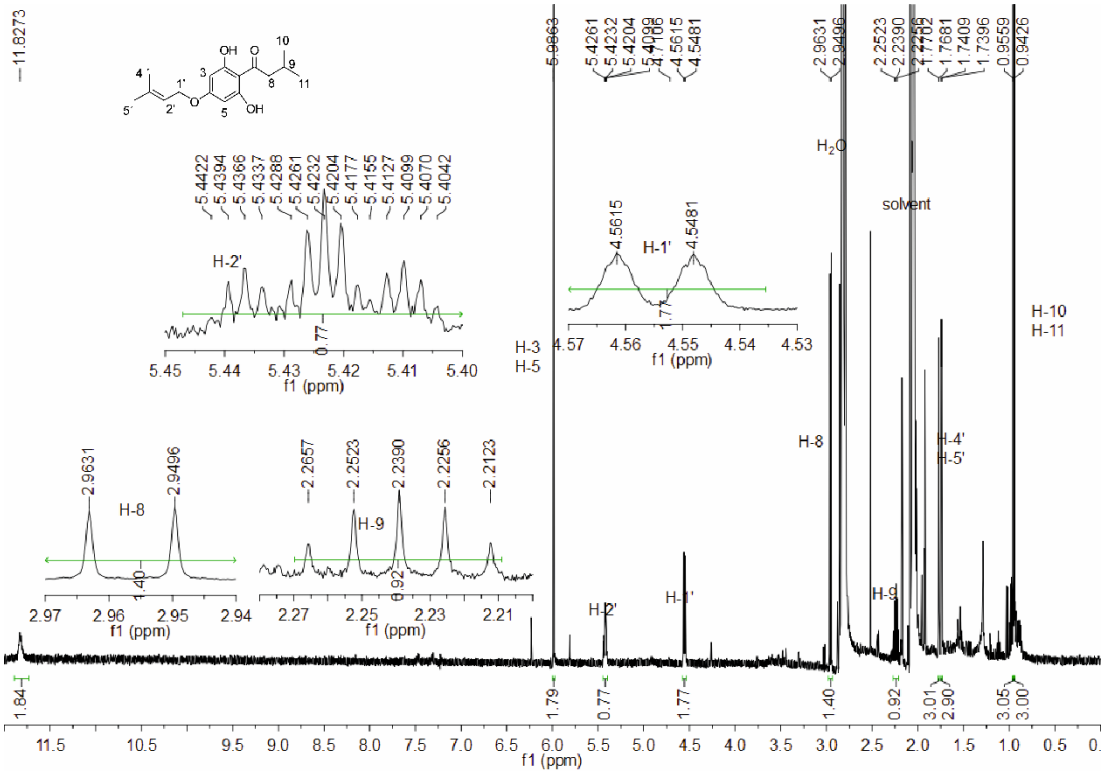

Figure S11. ^{1}H-NMR spectrum of **2D2** in acetone-D_6, 500 MHz.

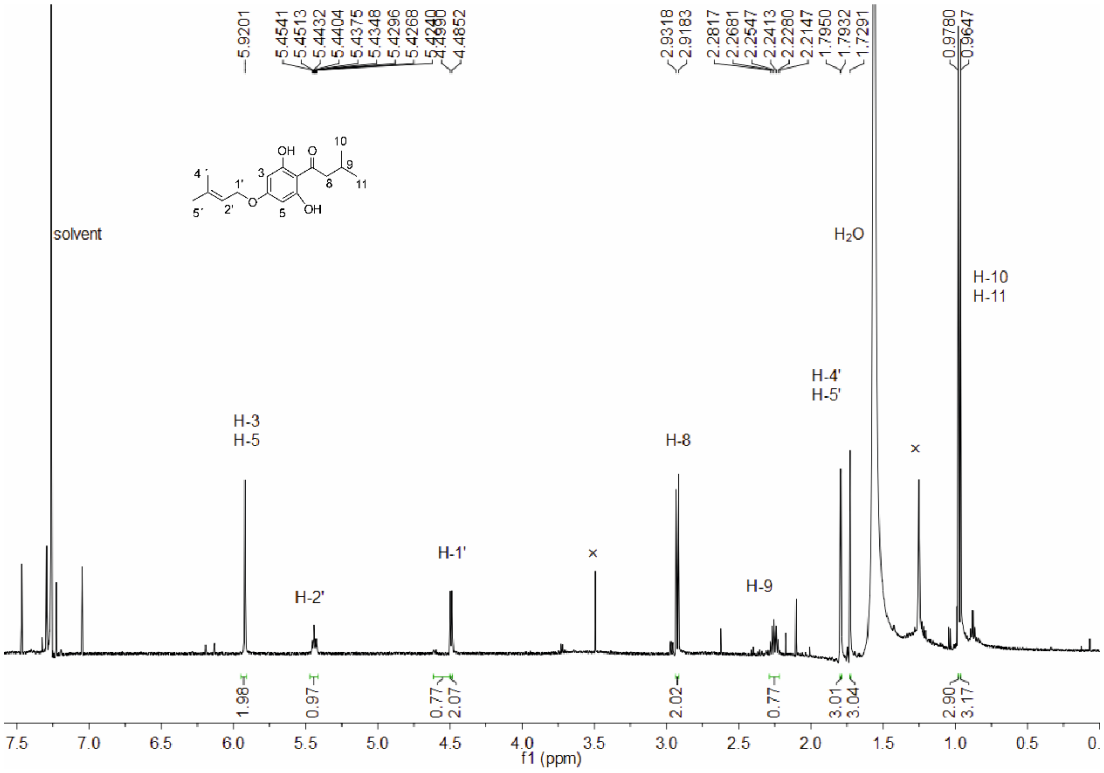

Figure S12. ^{1}H-NMR spectrum of **2D2** in $CDCl_3$, 500 MHz.

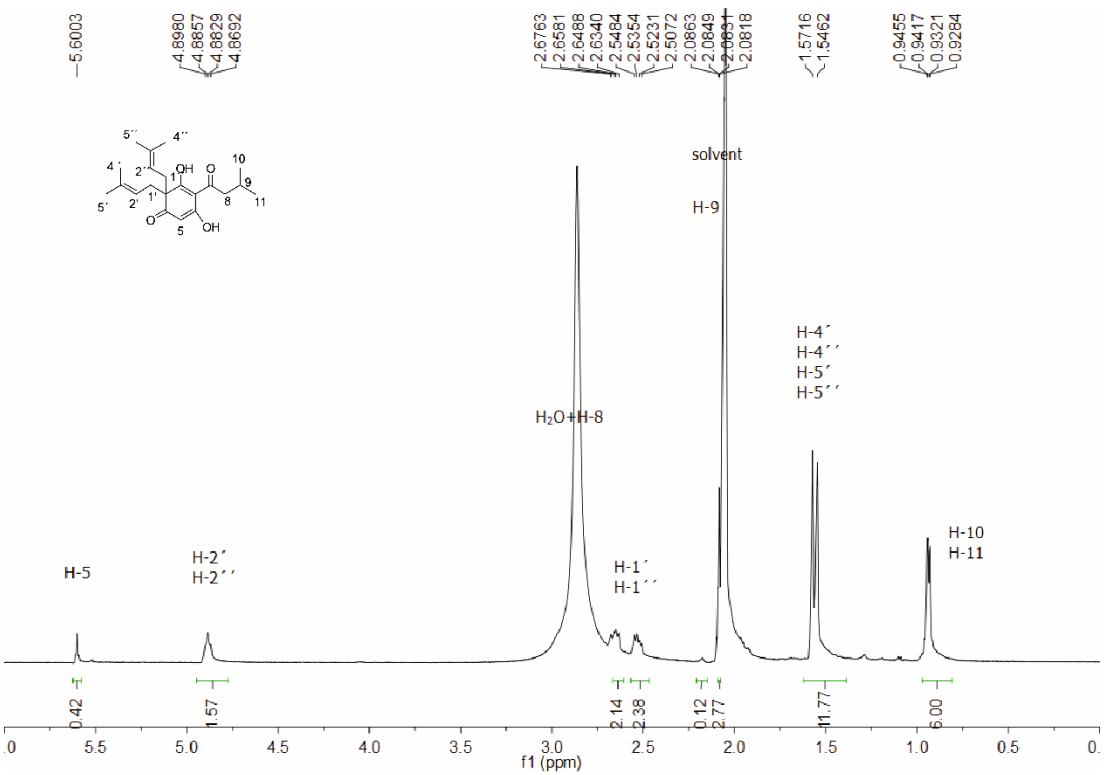

Figure S13. ^{1}H-NMR spectrum of **2D3** in acetone-D_6, 500 MHz.

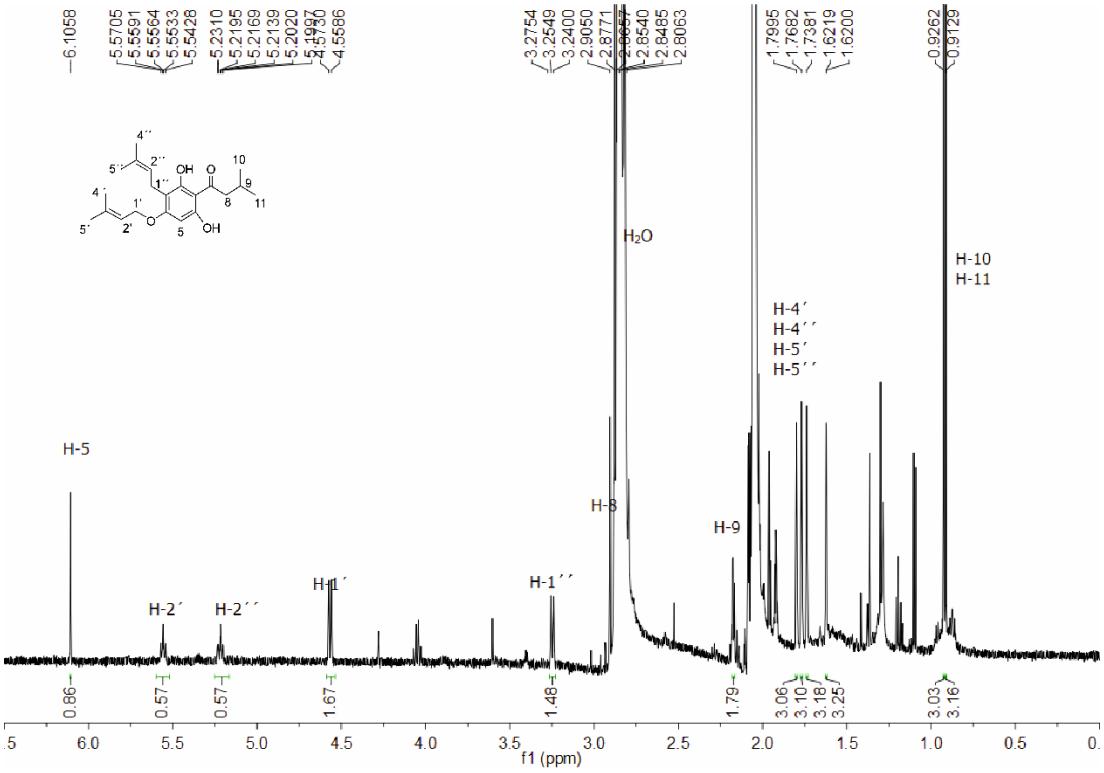

Figure S14. ^{1}H-NMR spectrum of **2D4** in acetone-D_6, 500 MHz.

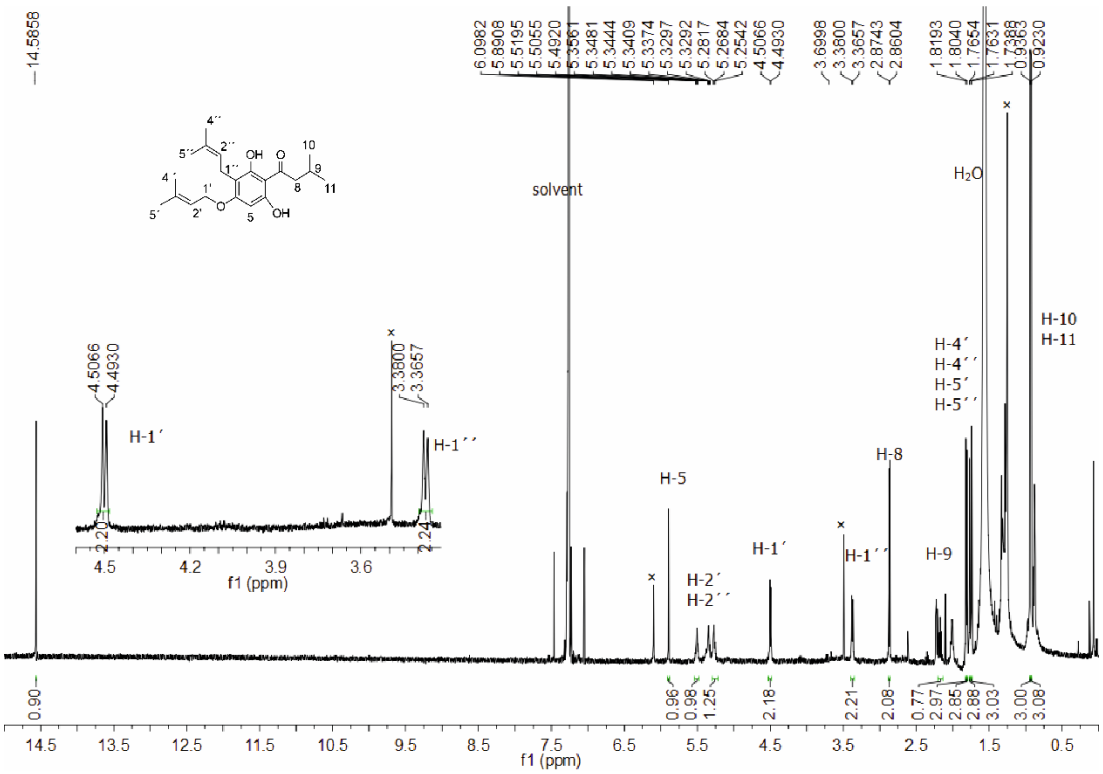

Figure S15. ^{1}H-NMR spectrum of **2D4** in $CDCl_3$, 500 MHz.

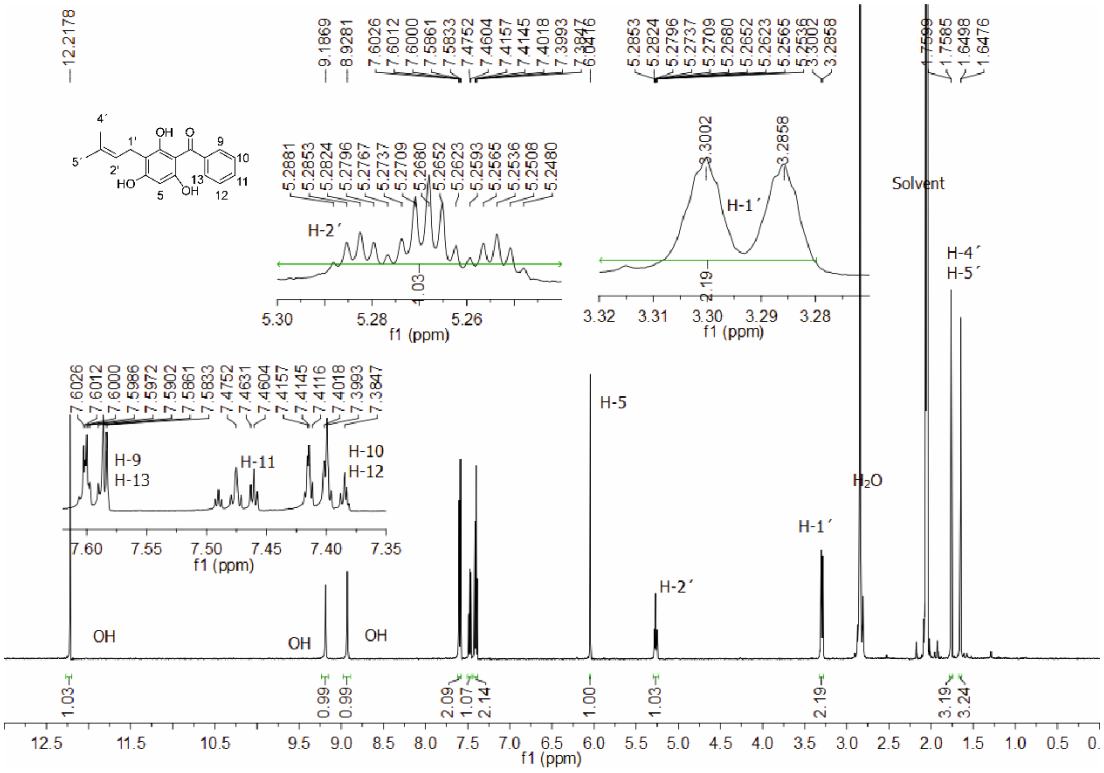

Figure S16. ^{1}H-NMR spectrum of **3D1** in acetone-D_6, 500 MHz.

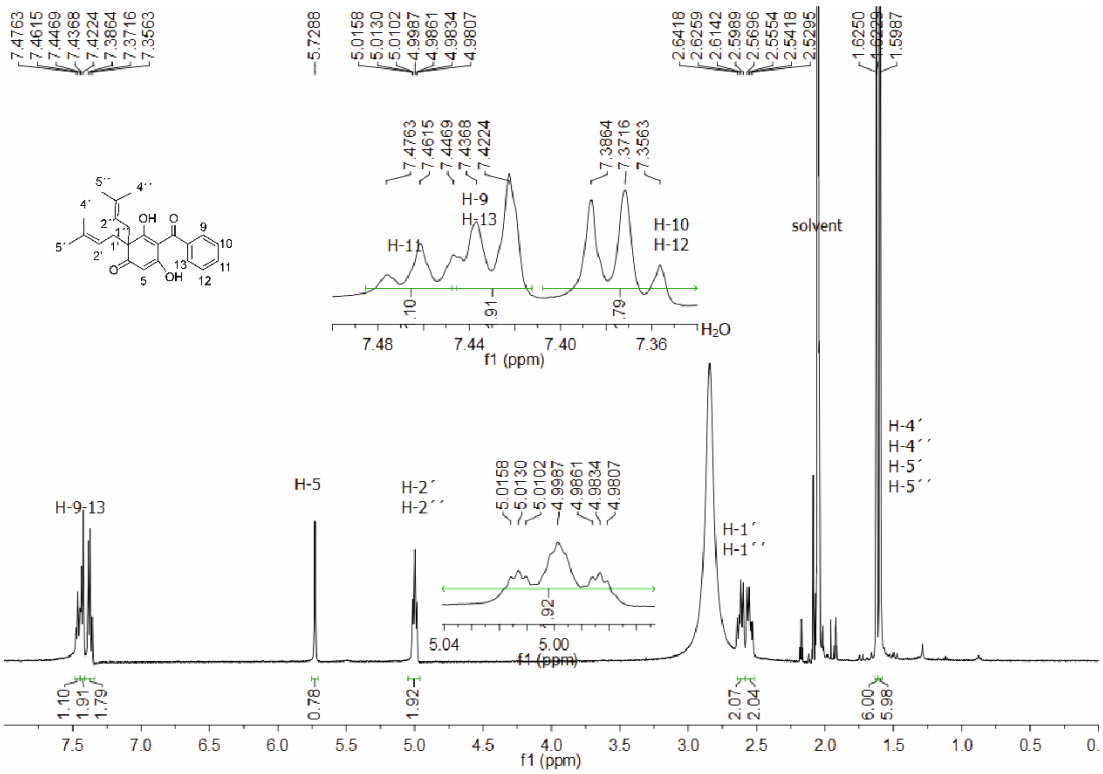

Figure S17. ^{1}H-NMR spectrum of **3D3** in acetone-D_6, 500 MHz.

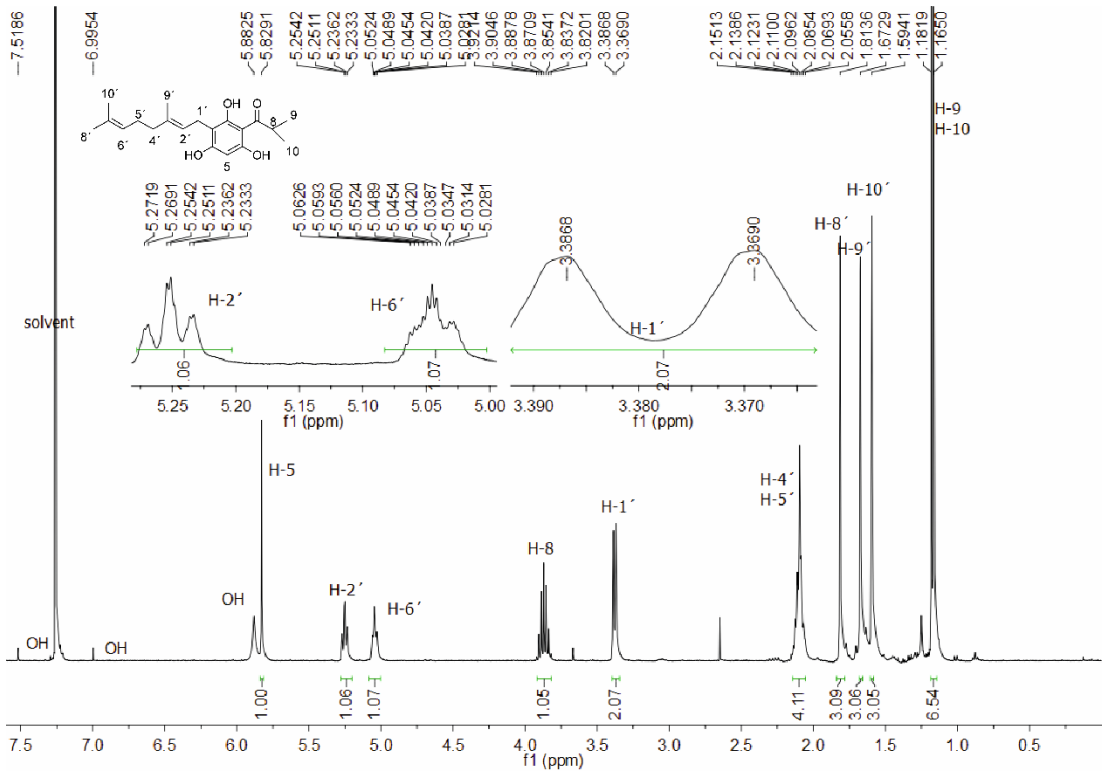

Figure S18. ^{1}H-NMR spectrum of **1G1** in $CDCl_3$, 400 MHz.

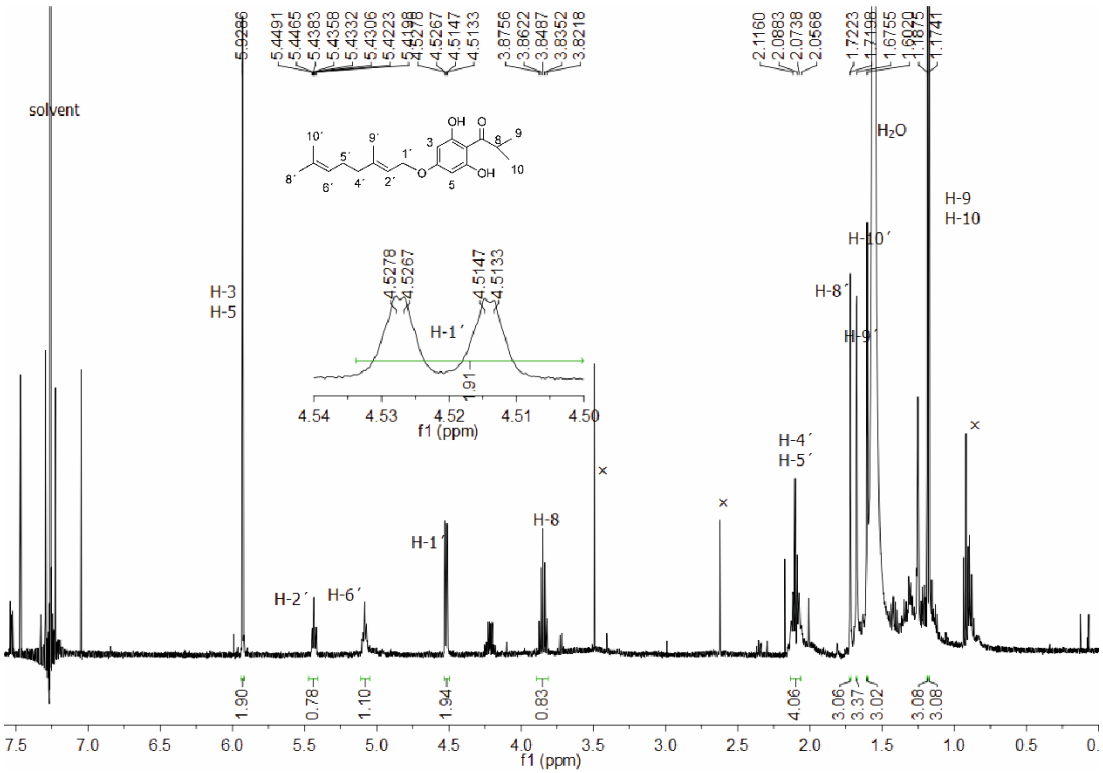

Figure S19 ^{1}H-NMR spectrum of **1G2** in $CDCl_3$, 500 MHz.

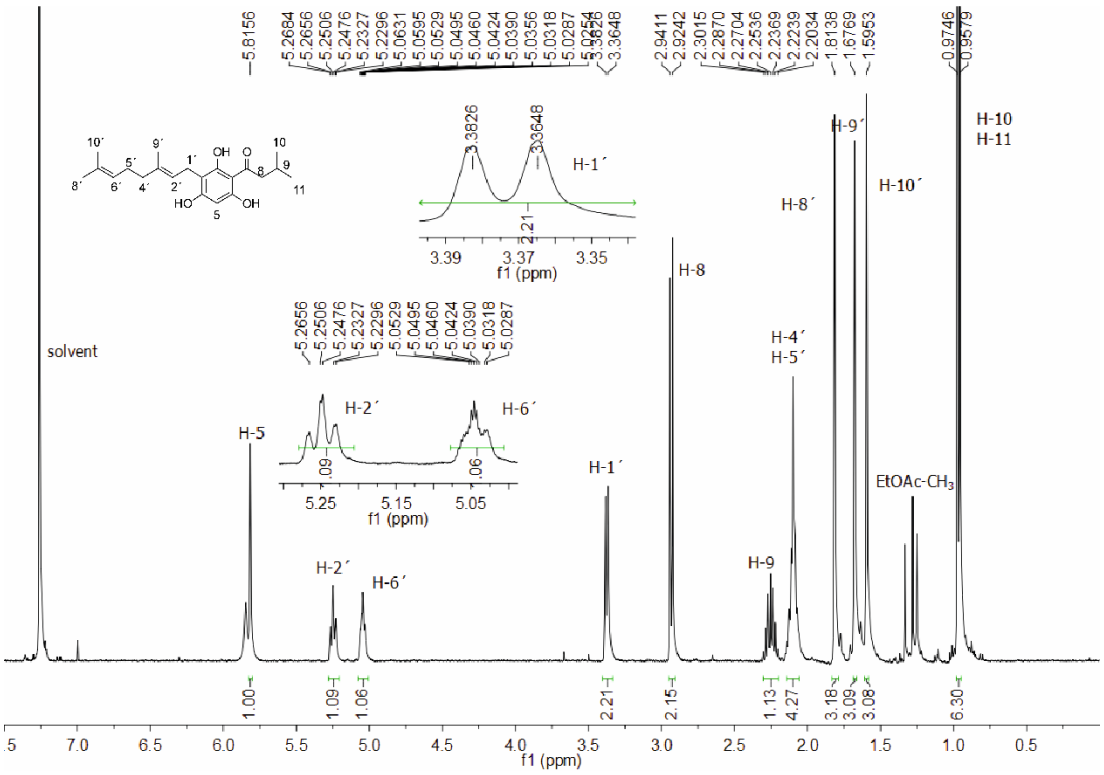

Figure S20. ^{1}H-NMR spectrum of **2G1** in $CDCl_3$, 400 MHz.

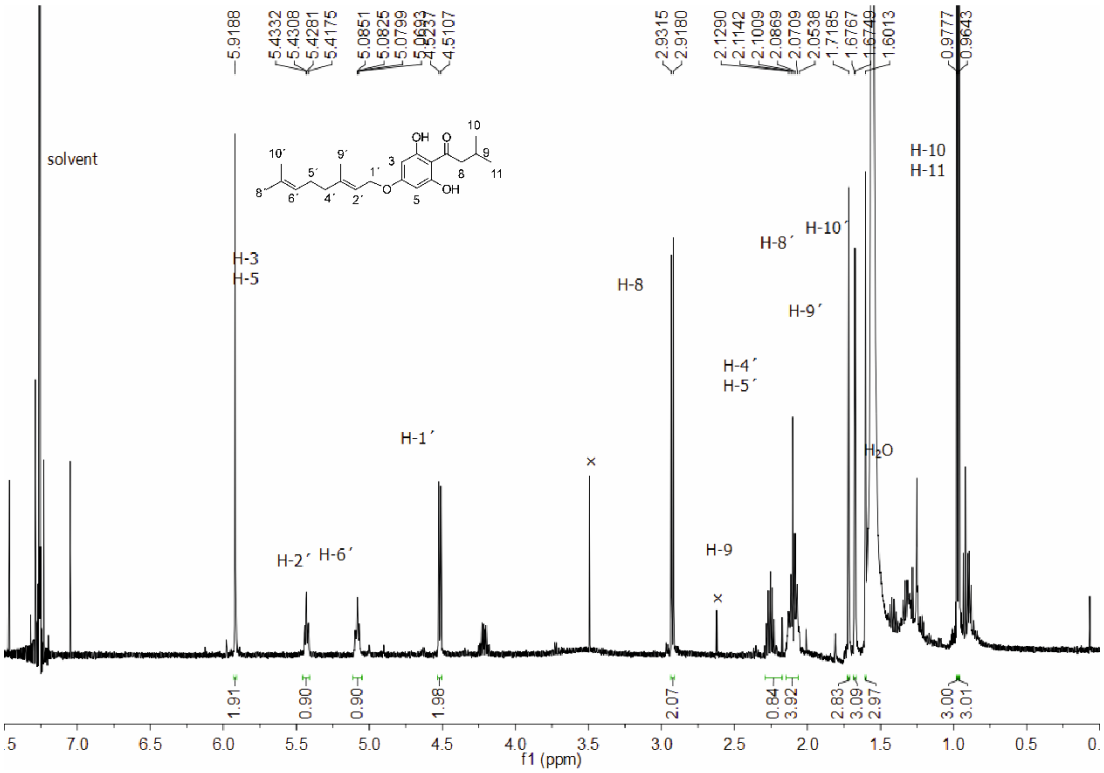

Figure S21. ^{1}H-NMR spectrum of **2G2** in $CDCl_3$, 500 MHz.

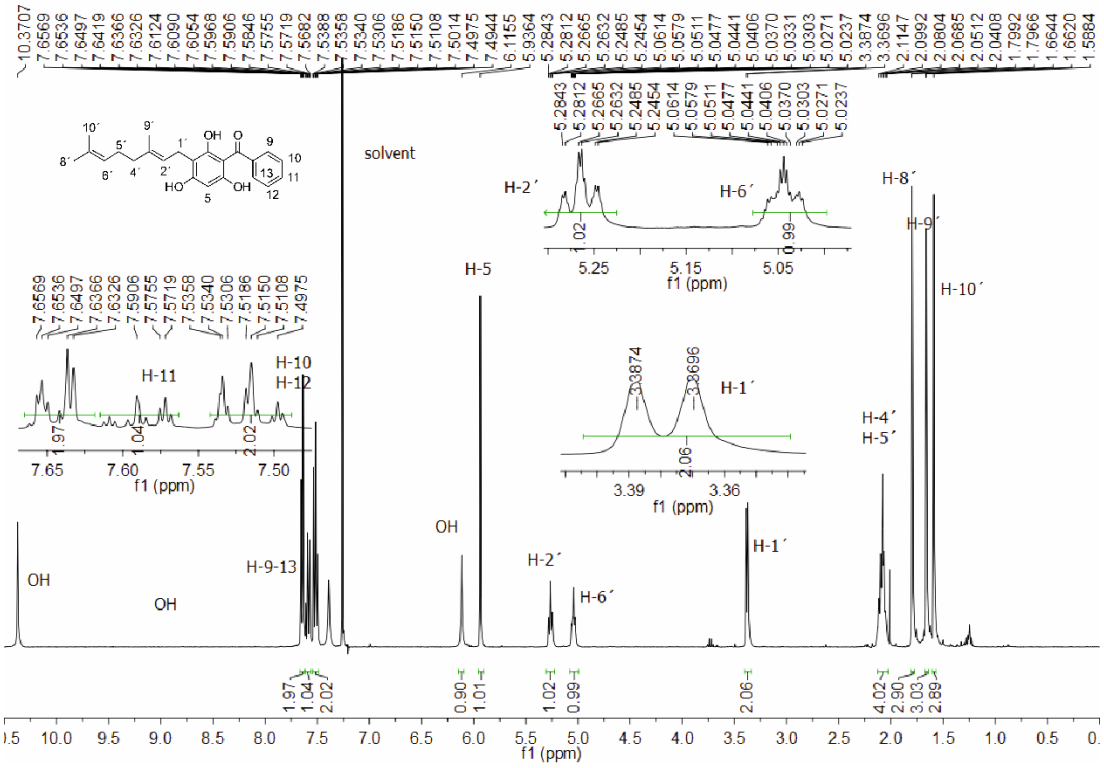

Figure S22. ^{1}H-NMR spectrum of **3G1** in $CDCl_3$, 400 MHz.

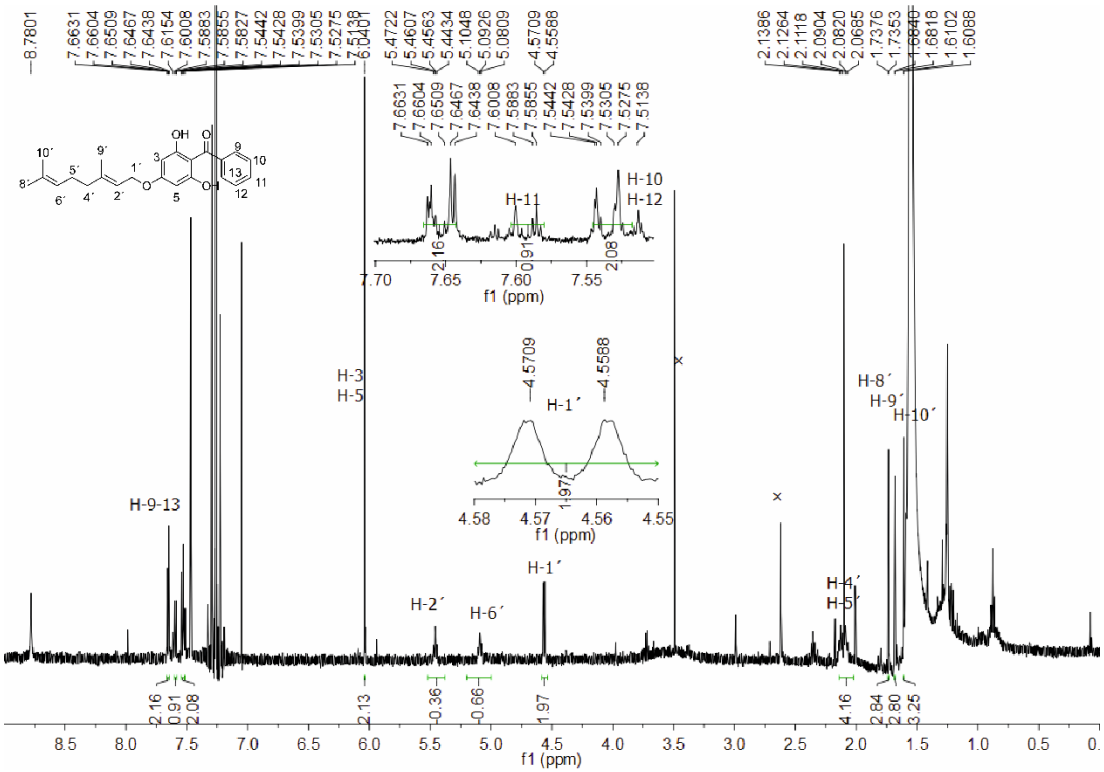

Figure S23. ^{1}H-NMR spectrum of **3G2** in $CDCl_3$, 500 MHz.

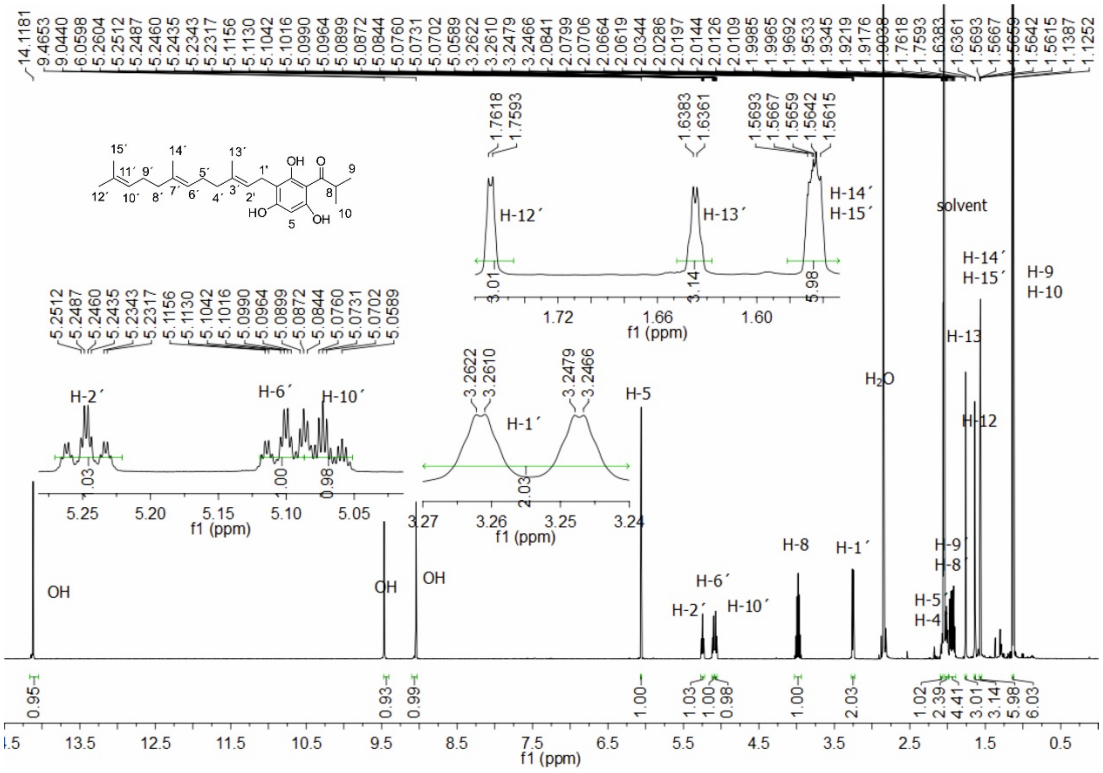

Figure S24. ^{1}H-NMR spectrum of **1F1** in acetone-D_6, 500 MHz.

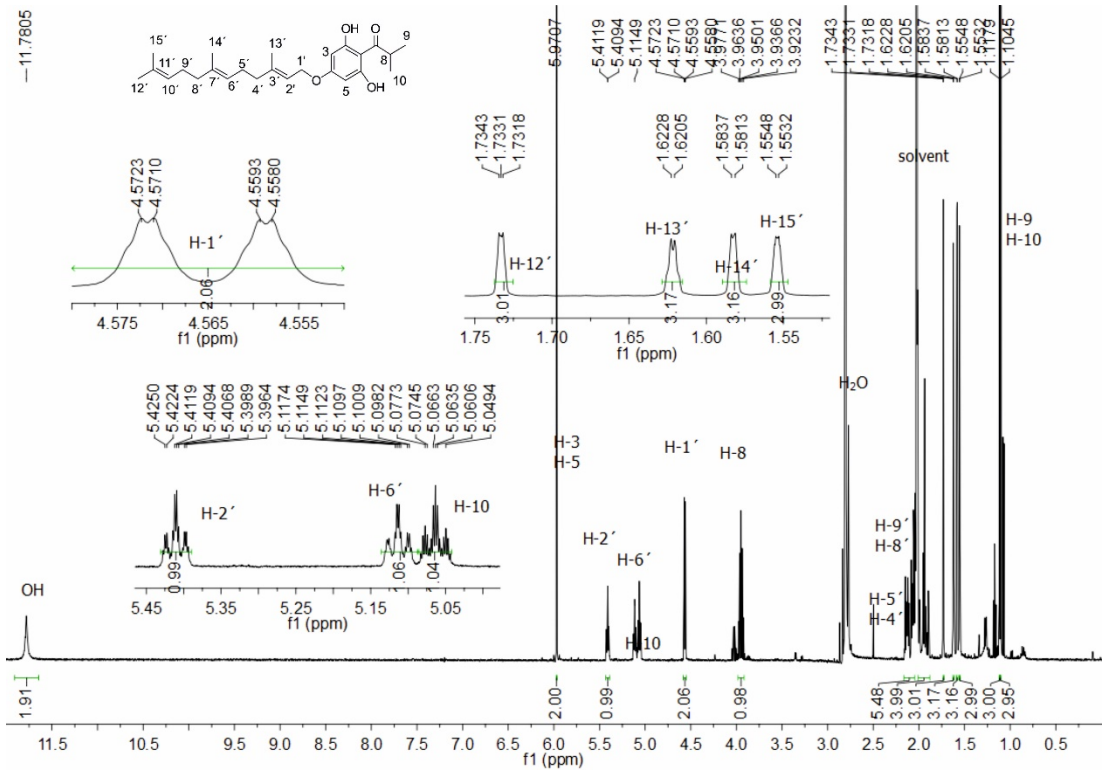

Figure S25. ^{1}H-NMR spectrum of **1F2** in acetone-D_6, 500 MHz.

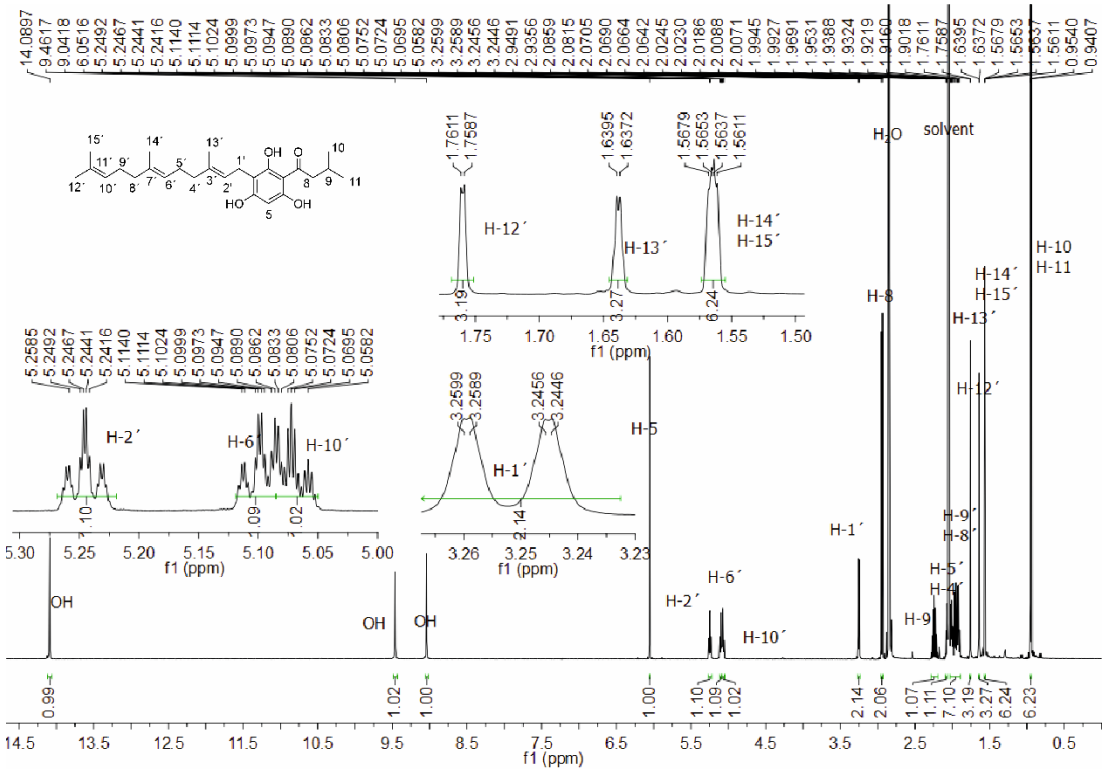

Figure S26. ^{1}H-NMR spectrum of **2F1** in acetone-D_6, 500 MHz.

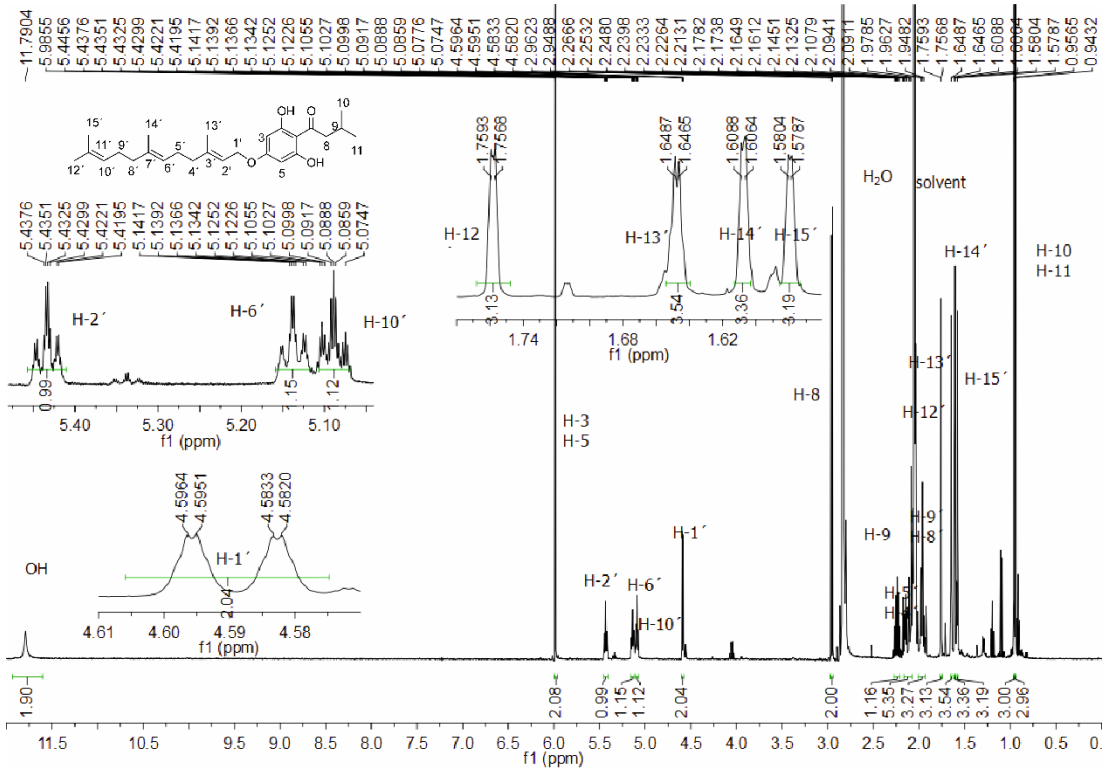

Figure S27. ^{1}H-NMR spectrum of **2F2** in acetone-D_6, 500 MHz.

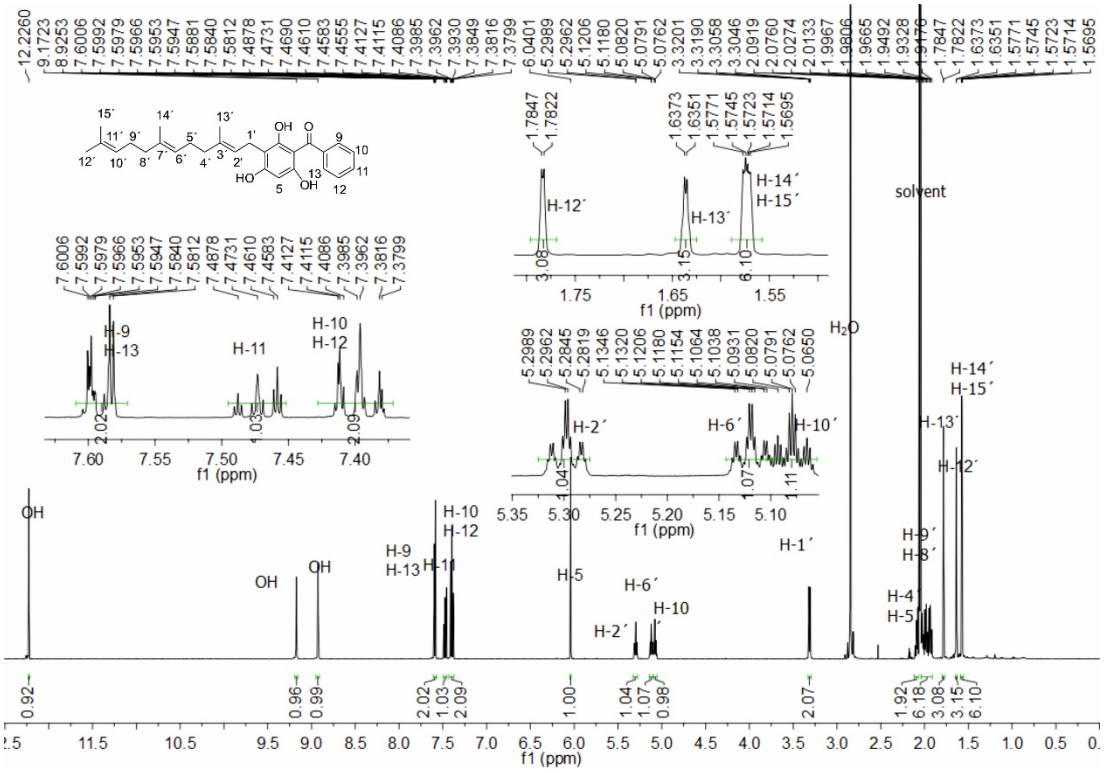

Figure S28. [1]H-NMR spectrum of **3F1** in acetone-D_6, 500 MHz.

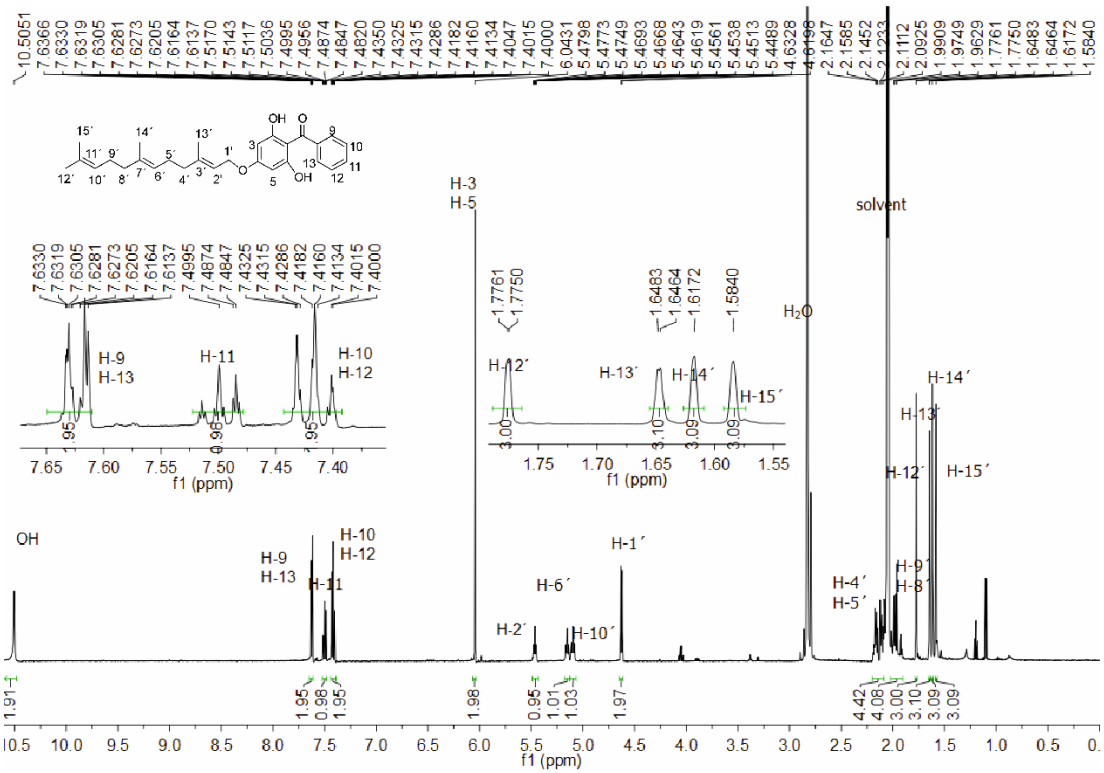

Figure S29. [1]H-NMR spectrum of **3F2** in acetone-D_6, 500 MHz.

X. Dependence of product formation of AtaPT reactions on incubation time.

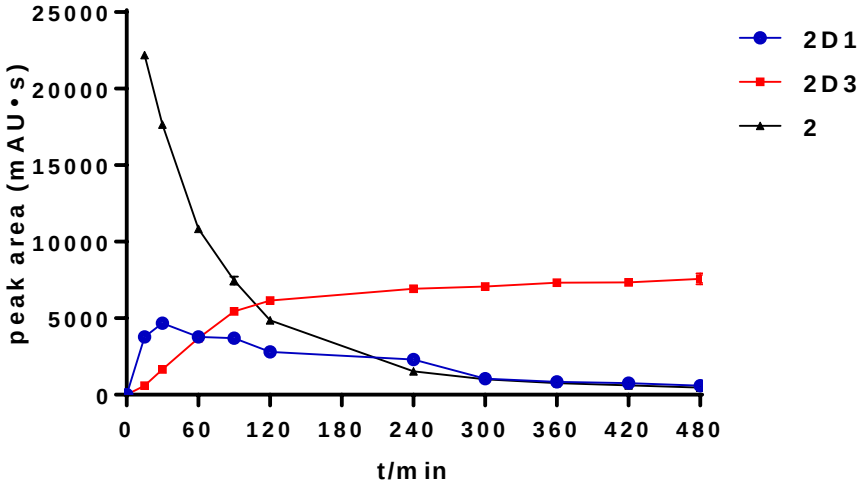

Figure S30. Time dependence of the product formation of AtaPT reaction with **2** and DMAPP.

The enzyme assays (100 µL) contained 0.5 mM of **2**, 5 mM of $CaCl_2$, 2 mM of DMAPP, 1.2% of glycerol, 5% of DMSO, and 50 µg of the purified recombinant protein in 50 mM Tris-HCl, pH 7.5.

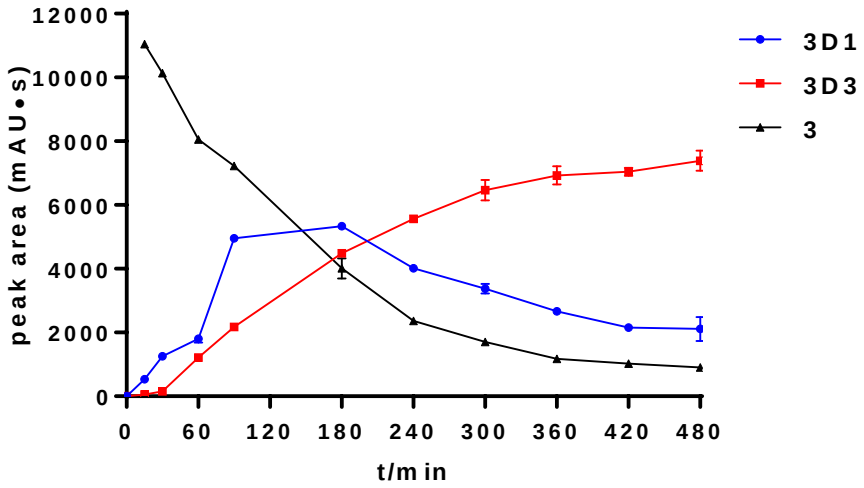

Figure S31. Time dependence of the product formation of AtaPT reaction with **3** and DMAPP.

The enzyme assays (100 µL) contained 0.5 mM of **3**, 5 mM of $CaCl_2$, 2 mM of DMAPP, 1.2% of glycerol, 5% of DMSO, and 50 µg of the purified recombinant protein in 50 mM Tris-HCl, pH 7.5.

XI. Figures of kinetic parameters

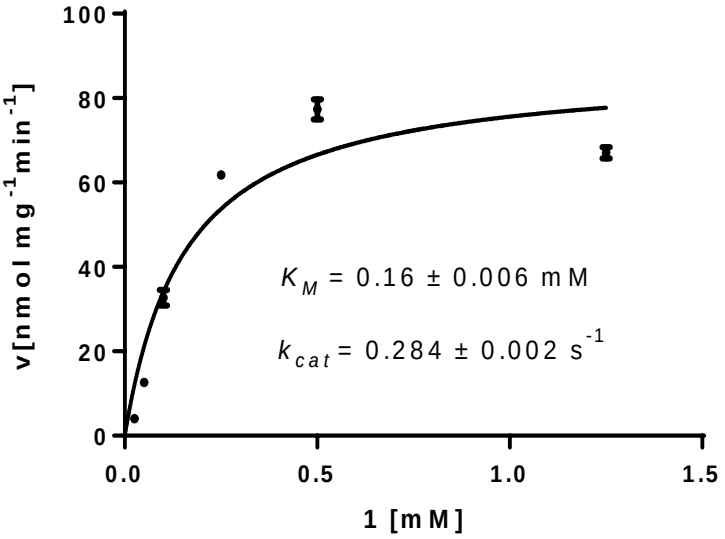

Figure S32. Determination of the kinetic parameters of the AtaPT reaction toward **1** in the presence of DMAPP.

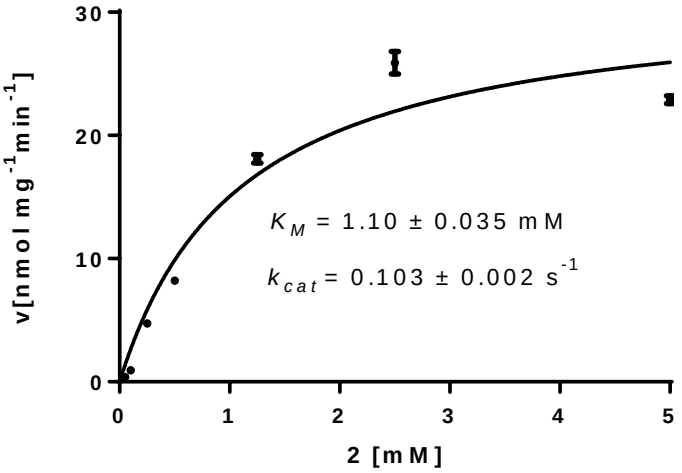

Figure S33. Determination of the kinetic parameters of the AtaPT reaction toward **2** in the presence of DMAPP.

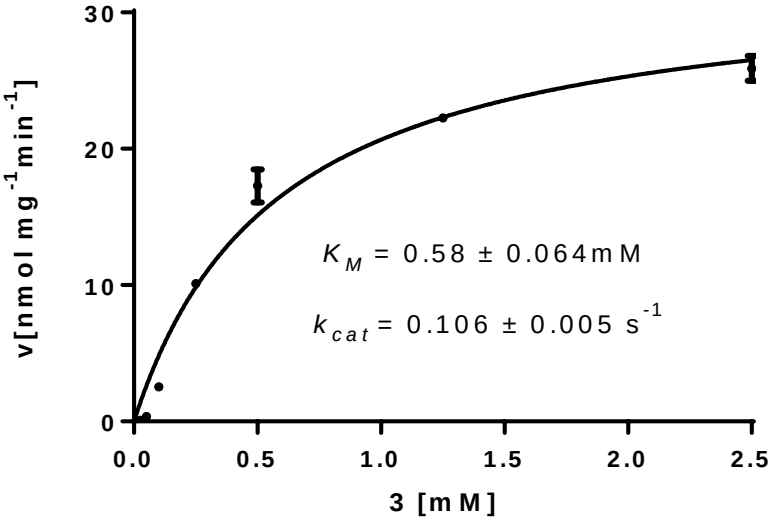

Figure S34. Determination of the kinetic parameters of the AtaPT reaction toward **3** in the presence of DMAPP.

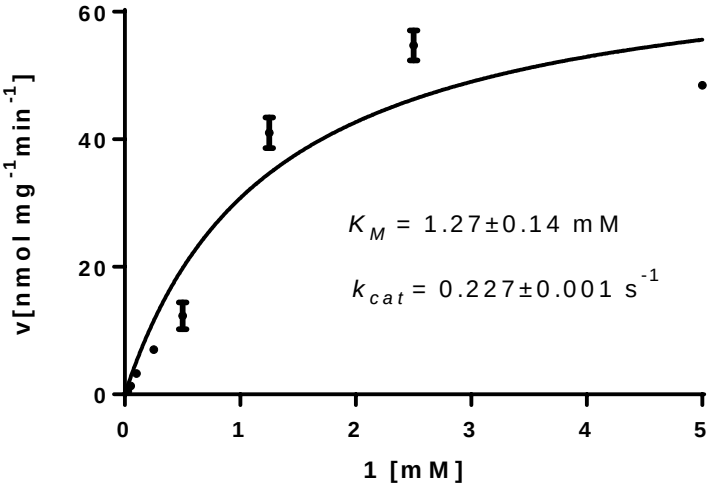

Figure S35. Determination of the kinetic parameters of the AtaPT reaction toward **1** in the presence of GPP.

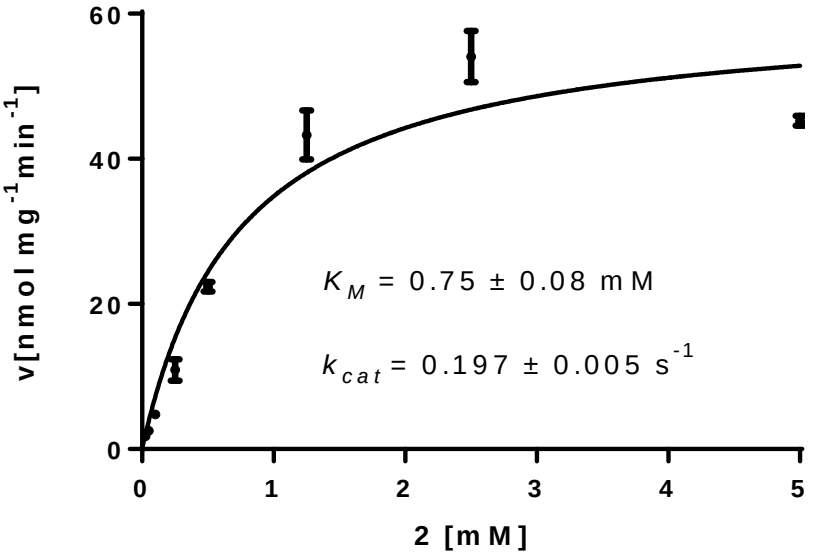

Figure S36. Determination of the kinetic parameters of the AtaPT reaction toward **2** in the presence of GPP.

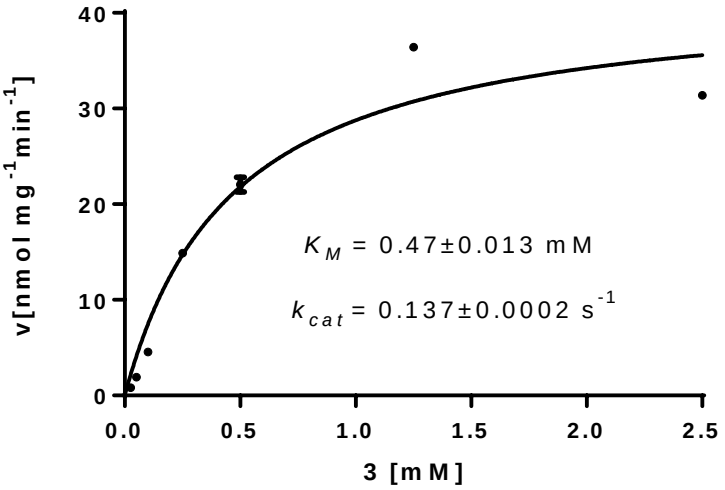

Figure S37. Determination of the kinetic parameters of the AtaPT reaction toward **3** in the presence of GPP.

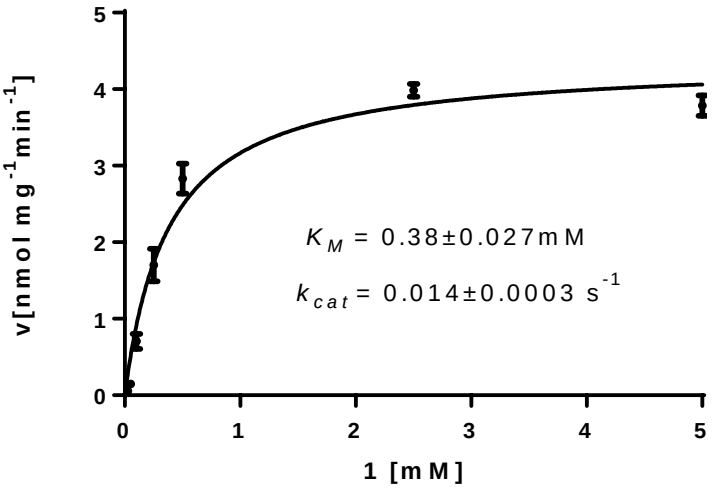

Figure S38. Determination of the kinetic parameters of the AtaPT reaction toward **1** in the presence of FPP.

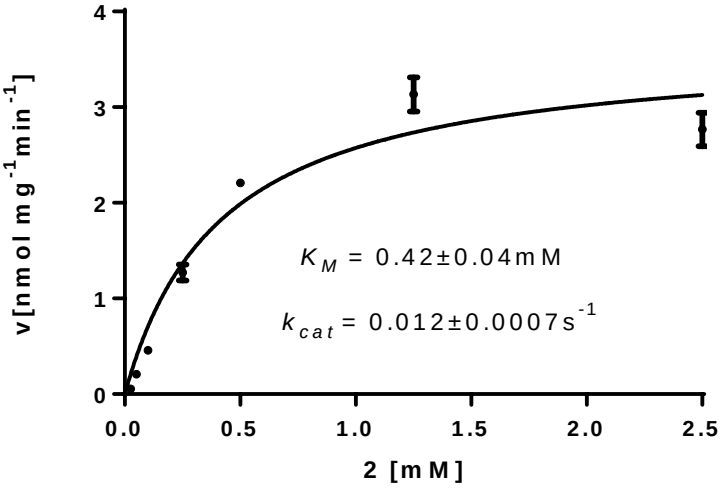

Figure S39. Determination of the kinetic parameters of the AtaPT reaction toward **2** in the presence of FPP.

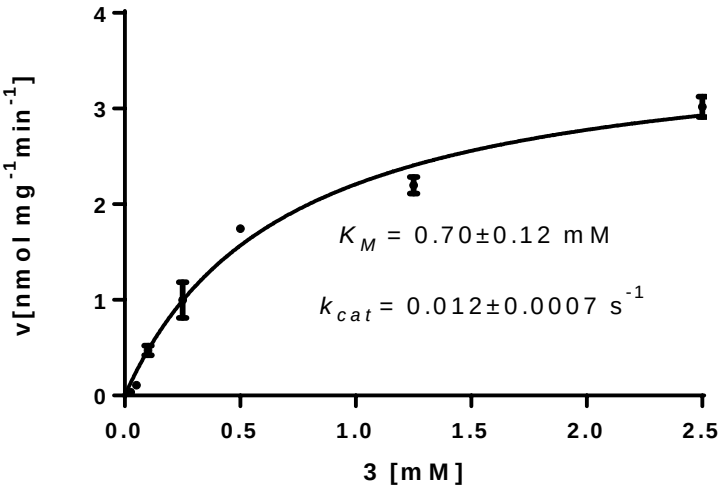

Figure S40. Determination of the kinetic parameters of the AtaPT reaction toward **3** in the presence of FPP.

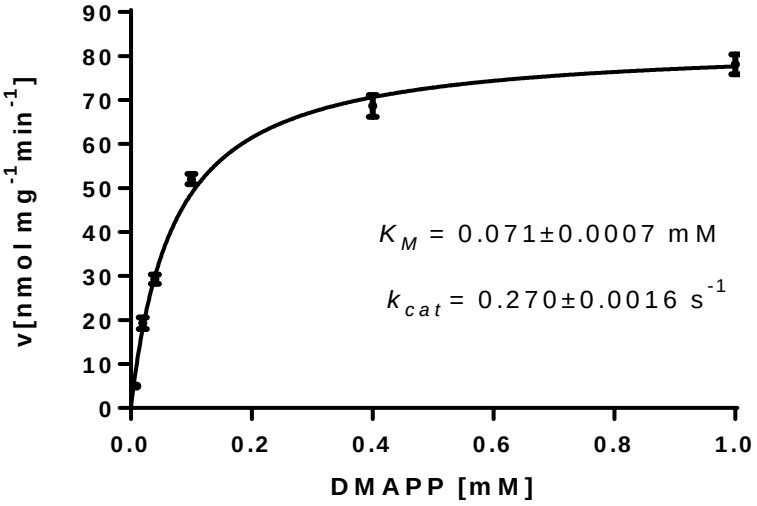

Figure S41. Determination of the kinetic parameters of the AtaPT reaction toward DMAPP with **1** as prenyl acceptor.

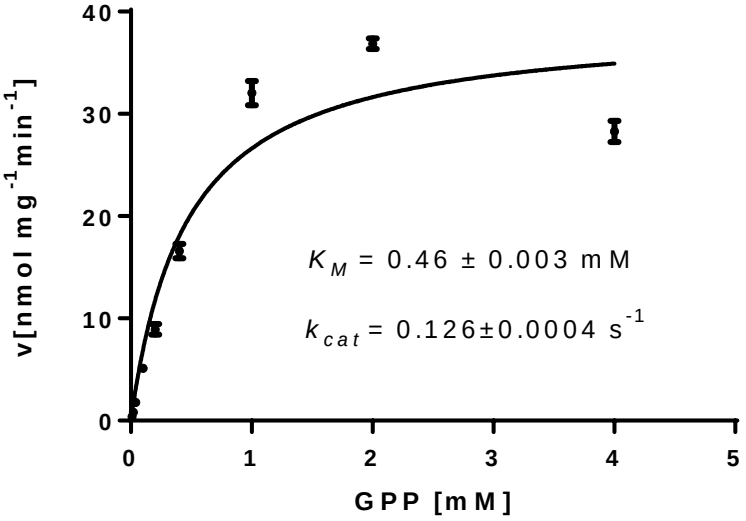

Figure S42. Determination of the kinetic parameters of the AtaPT reaction toward GPP with **3** as prenyl acceptor.